

International Materials Reviews

ISSN: (Print) (Online) Journal homepage: www.tandfonline.com/journals/yimr20

Ceramic-based electromagnetic wave absorbing materials and concepts towards lightweight, flexibility and thermal resistance

Wei Li, Zhaoju Yu, Qingbo Wen, Yao Feng, Bingbing Fan, Rui Zhang & Ralf Riedel

To cite this article: Wei Li, Zhaoju Yu, Qingbo Wen, Yao Feng, Bingbing Fan, Rui Zhang & Ralf Riedel (2023) Ceramic-based electromagnetic wave absorbing materials and concepts towards lightweight, flexibility and thermal resistance, International Materials Reviews, 68:5, 487-520, DOI: [10.1080/09506608.2022.2077028](https://doi.org/10.1080/09506608.2022.2077028)

To link to this article: <https://doi.org/10.1080/09506608.2022.2077028>



Published online: 06 Jun 2022.



Submit your article to this journal 



Article views: 2343



View related articles 



View Crossmark data 



Citing articles: 3 View citing articles 



Ceramic-based electromagnetic wave absorbing materials and concepts towards lightweight, flexibility and thermal resistance

Wei Li^b, Zhaoju Yu^a, Qingbo Wen^{b,c}, Yao Feng^b, Bingbing Fan^d, Rui Zhang^{d,e} and Ralf Riedel^b

^aCollege of Materials, Key Laboratory of High Performance Ceramic Fibers (Xiamen University), Ministry of Education, Xiamen, People's Republic of China; ^bDepartment of Materials and Earth Sciences, Technical University of Darmstadt, Darmstadt, Germany; ^cState Key Laboratory of Powder Metallurgy, Central South University, Changsha, People's Republic of China; ^dSchool of Materials Science and Engineering, Zhengzhou University, Henan, People's Republic of China; ^eProvincial Key Laboratory of Aviation Materials and Application Technology, Zhengzhou Institute of Aeronautics, Henan, People's Republic of China

ABSTRACT

Electromagnetic wave (EMW) absorbing materials have attracted much attention in recent years due to the dramatical increase of high-frequency electronic components and devices, which generate electromagnetic (EM) pollution and cause serious electromagnetic interference (EMI). Ceramics and associated (nano)composites are widely investigated as EMW absorbing materials because of their excellent mechanical properties, chemical/thermal stabilities, and oxidation/corrosion resistance. In addition to outstanding EMW absorbing performance, lightweight, flexibility and thermal resistance at high temperatures strongly affect their practical applications. Therefore, this review highlights the recent progress of advanced ceramic-based EMW absorbing materials by evaluating their vital EMW absorption parameters. First, the fundamentals of EMW absorption are briefly summarized, followed by the effects of phase/chemical composition, micro/nano structure, and morphology on the EMW absorbing performance and associated mechanisms. Furthermore, modern strategies for the preparation of lightweight, flexible and thermal resistant EMW absorbing materials are comprehensively reviewed. Finally, the perspectives of advanced-ceramics as EMW absorbing materials are discussed as well.

ARTICLE HISTORY

Received 18 November 2020
Accepted 5 May 2022

KEYWORDS

Ceramics; ceramic composites; electromagnetic wave absorption; dielectric loss; magnetic loss; lightweight; flexibility; high temperature

Introduction

History and recent developments of EMW absorption

Rapid developments in electromagnetic technologies and widespread applications of electronic devices result in plentiful electromagnetic radiations in the living space of human beings (Figure 1) [1–8], which generate serious negative effects on human's health and life. In addition, these electromagnetic radiations can also seriously interfere with the communication system and safety operation of many electronic devices, which cause threats to information security, especially in the medical, aerospace and marine fields. The concept of electromagnetic interference (EMI) was first proposed by the International Special Committee on Radio Interference in 1933, in Paris, which started up a profound influence on the world's rules and regulations related to EMI [9,10]. In 1970s, researchers and the scientific community were shocked by the harm of EM radiation on living beings, electronic systems/equipment and the entire environment. EMI originating either from natural sources (e.g. lightning, solar flares, and thunder) or artificial

equipment (e.g. radar, computers, and telecommunication systems) was therefore defined as a new type of pollution [10]. Since then, the shielding of EM radiation has become a universal concern all over the world, and many strict rules and regulations on controlling the EMI of electronic devices have been implemented. For example, in 1979, the Federal Communications Commission in U.S.A. imposed legal restrictions on EM radiation for all electronic devices and established limits for specific absorption rates of human beings. Up to now, the restrictions are still in effect. In Europe, due to public health considerations, the regulatory authorities developed special guidelines aimed at protecting children and other vulnerable people from EM radiation. They also established occupational laws to reduce the risk of EM exposure to pregnant women and people with medical implants [11–13]. Therefore, it is significantly important to seek out long-term solutions to protect human beings from EMI [14–20].

As one effective solution of this issue, EMW absorbing materials have attracted great interests in both academia and industry because they possess the ability to dissipate the EMW energy without

CONTACT Zhaoju Yu zhaojuyu@xmu.edu.cn College of Materials, Key Laboratory of High Performance Ceramic Fibers (Xiamen University), Ministry of Education, Xiamen 361005, People's Republic of China; Qingbo Wen wentsingbo@csu.edu.cn Department of Materials and Earth Sciences, Technical University of Darmstadt, Darmstadt 64283, Germany; State Key Laboratory of Powder Metallurgy, Central South University, Changsha 410083, People's Republic of China

© 2022 Institute of Materials, Minerals and Mining and ASM International Published by Taylor & Francis on behalf of the Institute and ASM International

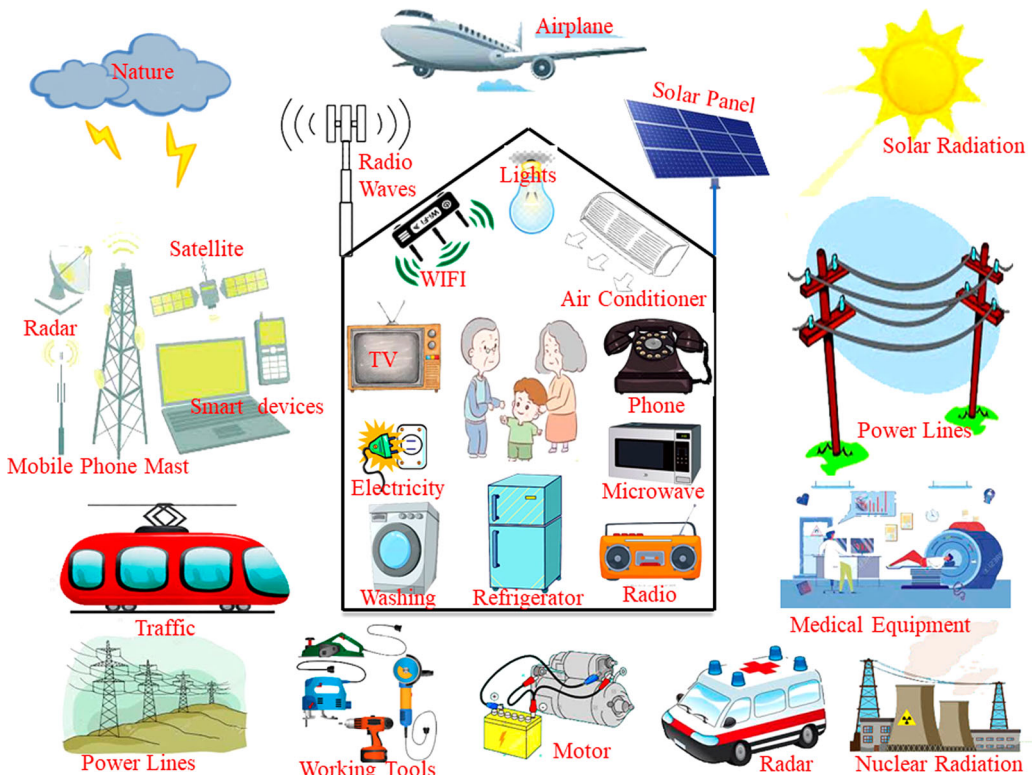


Figure 1. EMWs in the living space of human beings (www.hese-project.org).

secondary reflection. Therefore, a great number of novel EMW absorbers with excellent EMW absorbing performance have emerged [21–29]. As shown in the statistical data obtained from the Web of Science (Figure 2), the number of publications regarding EMW absorption increases year by year. In addition to outstanding EMW absorbing performance, lightweight, flexibility and thermal resistance at high temperatures are three other important technical demands for effective and practical applications of EMW absorbing materials, especially in the field of next-generation flexible electronic devices such as portable/

wearable electronics. The desired characteristics of an ideal EMW absorbing material are shown in Figure 3.

EMW absorbing materials can be classified into two categories according to their attenuation mechanisms, namely magnetic-loss-type materials (e.g. ferrites, magnetic metals, metallic alloys, and transition metal oxides) and dielectric-loss-type materials (e.g. carbon-based materials, conductive polymers, ceramics, and their composites) [30–32]. The magnetic-loss-type materials are mainly based on eddy current loss, natural resonance, domain-wall resonance, and exchange resonance. The dielectric-loss-type materials benefit from the conductivity and polarization

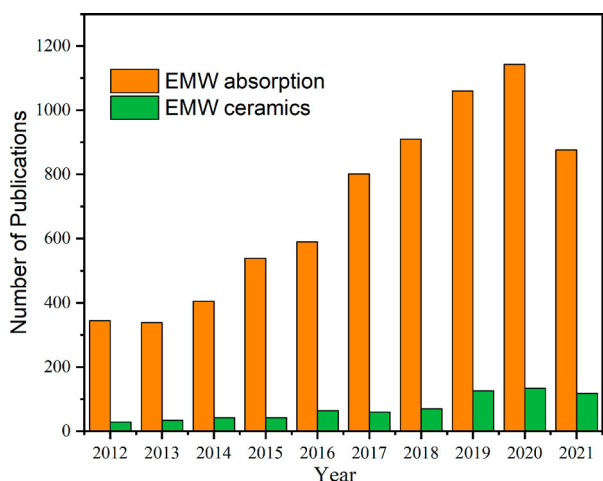


Figure 2. Number of publications resulting from a search with the topic 'Electromagnetic wave absorption' and 'Electromagnetic wave absorption and Ceramic' in 'All databases' on 'Web of Science' till 30th of August 2021.

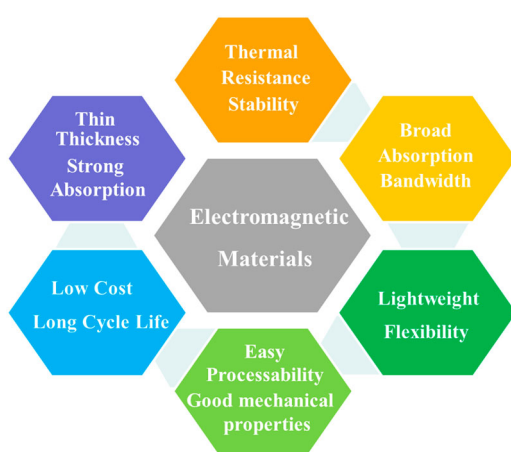


Figure 3. Desired characteristics of ideal EMW absorbing materials.

originating from the defects, interfaces and functional groups. Recently, EMW absorbing performance of magnetic materials and nanomaterials has been summarized by Kong et al. [33] and Wu et al. [31]. EMW absorption performance of conductive polymers and carbon-based composites has been reviewed by different researchers [14,15,34–37]. Yin et al. [38] summarized EMW absorbing properties of a small group of ceramics, namely Si-C-N-based ceramics and associated composites. However, there is no comprehensive review article focusing on ceramics and ceramic (nano)composites for EMW absorption applications in general. In the present review, we, therefore, focus on highlighting the EMW absorbing performance of ceramic-based materials as well as their absorbing mechanisms, influencing factors and requirements for practical applications.

Ceramic-based EMW absorbing materials

Ferrites [39–41] and other magnetic metal-containing ceramics [42–47] are promising candidate materials for EMW applications due to their advantages of magnetic loss. However, their intrinsic disadvantages, such as high density, poor mechanical strength, corrosion resistance, rigidity and poor processibility, restrict their extensive applications [48–54]. Compared with ceramic-based materials, their effective absorption bandwidth is mainly in the megahertz band width region because their permeability decreases rapidly with increasing frequency due to the eddy current loss. Moreover, their magnetic characteristics will be lost under temperatures higher than their Curie points. Therefore, these shortages restrict their universal applications in harsh environment (e.g. at elevated temperatures or in aggressive media) and in high frequency range (e.g. in GHz range).

Recently, polymer-based composites with high magnetic loss and/or conductivity are largely used as EMW absorption materials due to their easy

processability, low density, low cost, strong resistance to corrosion, lightweight, and broad effective absorption bandwidth [14,35,55–59]. However, polymer-based materials cannot be used at high temperatures as a result of their low melting points, limited thermal stability (only up to 400°C) and poor high-temperature mechanical properties.

Radar plots representing characteristics of EMW absorbing materials are given in Figure 4. Compared with magnetic metal-containing materials and polymers, ceramic-based systems exhibit high oxidation/corrosion resistance, excellent mechanical properties, high melting points and superior thermal stabilities, which make them to be used under severe environments. Therefore, a great number of ceramic-based materials with excellent EMA performance have been widely investigated, such as SiC [21,60–68], Si₃N₄ [69–73], Al₂O₃ [74–77], SiO₂ [78–81], SiOC [82–85], SiBCN [86–89], BaTiO₃ [90–93], Ti₃SiC₂ [94–97], BCN [98–100], and others. The number of publications of ceramic-based EMW absorption materials increases with an increasing amount of EMW absorption-related publications (Figure 2), and the number of publications since 2018 has exceeded the total number of 2012–2017, implying the importance of ceramics as potential candidate materials for EMW absorbing applications.

This article reviews the effects of phase/chemical compositions, micro/nano structures, and morphologies on the EMW absorbing performance and associated mechanisms. The advantages and limitations of ceramics and their composites, along with the approaches that are reported to overcome these limitations, are summarized. Besides, requirements for practical applications and expectation of ceramic-based EMW absorbing materials with lightweight, flexibility and thermal resistance are also discussed. Finally, the current challenges and perspectives are outlined. If there is no further remark, the EMW range of this review is mainly related to the microwave (MW) range between 2 and 18 GHz. This frequency range is operated by a large number of commonly used electronic devices, and most papers refer to it (Figure 5).

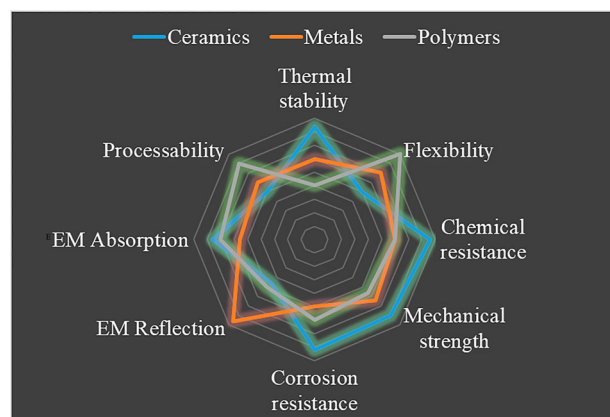


Figure 4. Radar plots representing characteristics of EMW absorbing materials.

Fundamentals of EMW absorption

Process of EMW absorption

Electromagnetic wave (EMW) is a radiation in the frequency range of 300 MHz–300 GHz. An EMW involves two important parts, namely, a magnetic field (H) and an electric field (E), which are perpendicular to each other. The direction in which EMWs propagate is perpendicular to the plane with the two field components. It is well known that the relationship between EMW frequency and wavelength can

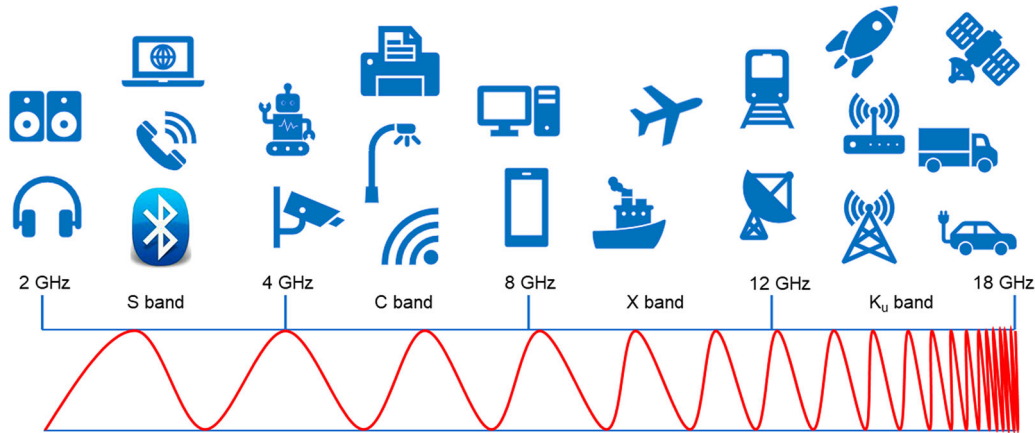


Figure 5. Electromagnetic spectrum and applications of EM bands in 2–18 GHz.

be expressed by formula (1):

$$c = \lambda f = \frac{1}{\sqrt{\epsilon_0 \mu_0}} \quad (1)$$

where f is the wave frequency, λ is the wavelength, c is the speed of the EMW in free space, ϵ_0 represents free space permittivity and μ_0 refers to the free space permeability. In a specific medium, relative complex permittivity (ϵ_r) and permeability (μ_r) can be expressed as $\epsilon_r = \epsilon' - j\epsilon''$ and $\mu_r = \mu' - j\mu''$, respectively, which determine the propagating behaviour of an EMW in materials. ϵ' and μ' are the real part of permittivity and permeability, which represent the storage capability of electric and magnetic energy, respectively. ϵ'' and μ'' are the imaginary part of permittivity and permeability, which describe the energy dissipation capability of the materials during the interaction with EMWs.

As shown in Figure 6, the incident EMW (E_I) is divided into four parts after entering the absorbers, namely, first reflection (E_{IR}), multiple-internal reflections (E_{2R}), absorption (E_A), and transmission (E_T). The ratio of E_I and E_A depends on the impedance matching, which is a decisive factor whether most

incident EMWs E_I can propagate into the absorbers. If the impedance is mismatched, most of the incident EMWs will be reflected at the interface between the free space (or air) and absorbing material, even though they exhibit high dielectric/magnetic loss. Therefore, good impedance matching is the prerequisite of effective EMW absorbers. In theory, the characteristic impedance values of EM absorbing materials should be close to that of the free space (377Ω) to reduce the reflection on the surface of the absorbing materials [103]. Recently, a delta-function method regulating the impedance matching degree of EMW absorbers has been proposed by Ma et al. [104] as follows:

$$|\Delta| = \sinh^2(Kfd) - M \quad (2)$$

where $|\Delta|$ refers to the impedance mismatch degree, K and M are determined by the following Equations (3) and (4), respectively.

$$K = \frac{4\pi\sqrt{\mu'\epsilon'} \cdot \sin \frac{\delta_e + \delta_m}{2}}{c \cdot \cos\delta_e \cos\delta_m} \quad (3)$$

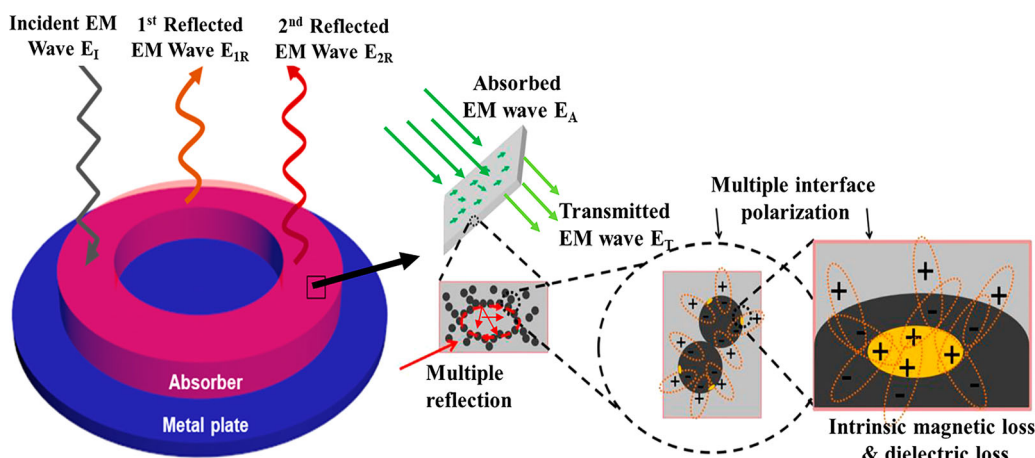


Figure 6. Schematic of EMW absorbing mechanisms [101,102].

$$M = \frac{4\mu' \epsilon' \cos \delta_e \cos \delta_m}{(\mu' \cos \delta_e - \epsilon' \cos \delta_m)^2 + \left[\tan \left(\frac{\delta_m - \delta_e}{2} \right) \right]^2 (\mu' \cos \delta_e + \epsilon' \cos \delta_m)^2} \quad (4)$$

With regard to Equations (3) and (4), c is the velocity of light, δ_e and δ_m are determined from the dielectric and magnetic dissipation factors $\tan \delta_e = \frac{\epsilon''_r}{\epsilon'_r}$ and $\tan \delta_m = \frac{\mu''_r}{\mu'_r}$. The aforementioned, ϵ'_r , μ'_r , ϵ''_r and μ''_r are the real part of permittivity and permeability, the imaginary part of permittivity and permeability, respectively. It is regarded as a good impedance matching when the $|\Delta|$ values are close to zero ($|\Delta| < 0.4$).

As mentioned before, the intensity of the EMWs penetrating into a material is governed by the impedance of the medium and material. Moreover, the strength of the transmitted EMWs drops exponentially with the increase of the penetrating depth. The depth at which the strength of EMW is equal to $\frac{e}{e} = 0.37$ of that of the incident wave is defined as skin depth δ , which is expressed by Equation (5) [105],

$$\delta = \sqrt{\frac{1}{\pi \mu_0 f \mu_r \sigma}} \quad (5)$$

According to Equation (5), δ will drop inversely with the increase of the electrical conductivity (σ), vacuum permeability (μ_0), relative magnetic permeability (μ_r) and frequency (f). Thus, the increase in the frequency and conductivity/permeability of the materials enhances reflection rather than absorption.

EMW absorbing mechanisms

Since EMWs consist of two components, magnetic and electric field, EMW absorbing materials can be classified into two categories: dielectric-loss type and magnetic-loss type absorbing materials. The absorbing mechanisms of the EMW absorbing materials can be understood by measuring their dielectric and magnetic properties.

Dielectric mechanism

Dielectric loss ability is primarily governed by ohmic loss and polarization loss [106–108]. Furthermore, the polarization loss can be caused by electronic polarization, ionic polarization, dipole orientation polarization, and interfacial polarization (space charge polarization) [109,110]. The dipole orientation and ionic polarization are attributed to the bound charges in the material, and the former is usually related to defects and residual groups in the dielectric medium. However, the dipoles cannot move freely as electrons under an external electric field due to the restriction on the defects and residual groups. The dipoles cannot

reorient swiftly enough to respond to the applied electric field under a high-frequency alternating electric field. Therefore, ϵ' and ϵ'' values begin to decrease and produce typical frequency dispersion behaviours. Ionic polarization and electronic polarization are easily excluded from EMW absorption because they usually occur in the higher frequency region (10³–10⁶ GHz) [111–113]. Interfacial polarization always arises from space charges that accumulate and unevenly distribute at the interface of two different materials, which will generate a macroscopic electric moment and can deplete the EMW energy effectively [36]. The polarization relaxation process can be described by a Cole–Cole semicircle corresponding to Debye dipole relaxation theory, and the relationship between ϵ' and ϵ'' can be described according to Equation (6) [114,115]:

$$\left(\epsilon' - \frac{\epsilon_s + \epsilon_\infty}{2} \right)^2 + (\epsilon'')^2 = \left(\frac{\epsilon_s - \epsilon_\infty}{2} \right)^2 \quad (6)$$

where ϵ_s represents the static dielectric permittivity and ϵ_∞ refers to the relative dielectric permittivity. The plot of ϵ' versus ϵ'' is a single semicircle related to a Debye relaxation process, which is called the Cole–Cole semicircle. For composites, more than one semicircle may be detected because of more than one Debye relaxation (or polarization mechanisms) occur. For example, Figure 7(a,b) displays typical plots of ϵ' versus ϵ'' of pure ZrB₂ and ZrN_{0.4}B_{0.6}/SiC, respectively [65]. As can be seen, pure ZrB₂ only presents one obvious Cole–Cole semicircle, which is derived from the Debye relaxation process of itself, while the ZrN_{0.4}B_{0.6}/SiC composites display nine semicircles in the frequency range, which can be attributed to the contribution of the Debye relaxation processes of ZrB₂, SiC and ZrN_{0.4}B_{0.6} as well as the interfacial polarization induced by the interfaces between ZrB₂, SiC and ZrN_{0.4}B_{0.6}. Semicircle may not be observed for highly conducting materials, as the dielectric loss primarily comes from conduction loss. In this case, the imaginary part of the permittivity can be expressed by Equation (7) according to the free electron theory [22,107]:

$$\epsilon'' = \frac{\sigma}{2\pi f \epsilon_0} \quad (7)$$

where σ is the DC electrical conductivity, f is the microwave frequency, and ϵ_0 refers to the free space permittivity. It can be found that high electrical conductivity results in the enhancement of the imaginary part of the permittivity. That means the energy loss caused by electrical conductance (i.e. ohmic loss)

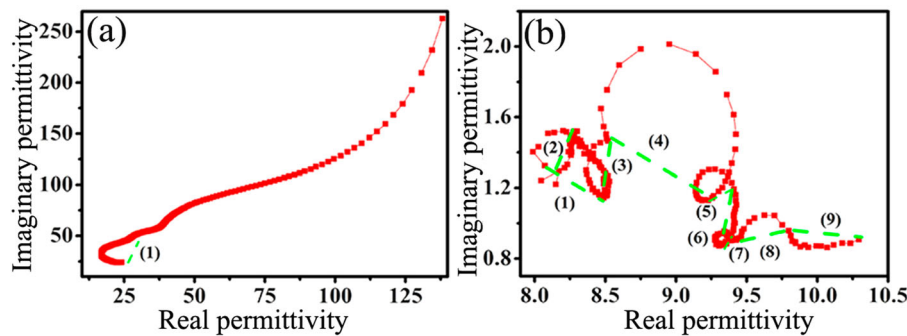


Figure 7. Typical Cole–Cole semicircles of (a) pure ZrB_2 and (b) $\text{ZrN}_{0.4}\text{B}_{0.6}/\text{SiC}$ (reprinted with permission from American Chemical Society) [65].

plays the main role in the dielectric loss. Furthermore, it can be seen that the real part of the permittivity decreases with the increase of the frequency, and this phenomenon is related to the presence of electric dipoles. While the frequency of the applied field increases, the dipoles in the materials cannot quickly adjust its direction to respond to the applied electric field, and as a result, the real part of the permittivity drops [116].

Magnetic mechanism

In general, the magnetic loss arises from hysteresis loss, domain wall resonance, natural resonance, residual loss and eddy current loss [117,118]. Among these mechanisms of magnetic loss, the hysteresis loss mainly comes from the strong EMW field, and domain wall resonance only occurs at much lower frequency (1–100 MHz) [119]. Thus, natural resonance and eddy current loss are regarded as two dominant factors that contribute to the magnetic loss. According to the natural resonance and eddy current loss theory [120], the natural resonance and eddy current loss can be expressed by the Equations (8), (9) and (10), respectively:

$$f_r = \frac{\gamma}{2\pi} H_e \quad (8)$$

$$H_e = \frac{4|k_1|}{3\mu_0 M_S} \quad (9)$$

$$C_0 = \frac{\mu''}{f(\mu')^2} = \frac{2}{3} \pi \sigma \mu_0 d^2 \quad (10)$$

where f_r is the resonance frequency, $\frac{\gamma}{2\pi}$ is the gyro-magnetic ratio, H_e is the effective anisotropy field, k_1 is the magnetic crystalline anisotropy co-efficient for a magnetic material, μ_0 is the vacuum permeability, d is the diameter of the magnetic nanoparticle, and M_S is the saturation magnetization, C_0 relates to the eddy current loss, μ' and μ'' represent the real part of permeability and the imaginary part of permeability, and σ is the electrical conductivity. As the small size effect and the confinement effect can lead

to an enhanced effective anisotropy, the natural resonance in frequency range can be regulated by decreasing the size of magnetic particles [121]. Moreover, the contribution of the eddy current to the magnetic loss can be estimated via analysing the dependence of $\mu''(\mu')^{-2}f^{-1}$ on the frequency. The eddy current loss is the only reason for the magnetic loss if the $\mu''(\mu')^{-2}f^{-1}$ value keeps constant with the change of frequency [122].

It is known from Equation (10) that the particle size of the materials plays a key role in determining the eddy current loss. In theory, a strong eddy current can generate a skin effect in case the particle size surpasses a critical value, which leads to a part of the loss of the internal magnetic field and consequently to a degraded relative complex permeability. Therefore, the particle size of the materials has an important influence on the EMW absorbing performance [123,124].

Evaluating methods of EMW absorbing performance

Generally, the absorption performance of EMW absorbing materials can be assessed by a vector network analyser (VNA) based on four methods: (1) Transmission-Line Technique (including co-axial transmission line method and waveguide method; (2) Bistatic Naval Research Laboratory Arch Measurement Method; (3) Free-Space Method; (4) Reverberation Chamber Method [125]. Evaluating methods of the EMW absorbing performance are designed to measure the power of the incident wave and the transmitted wave when the EMWs pass through the materials. The absorption capacity (A) is defined as the ratio between absorbed power (P_A) and incident power (P_I), $A = P_A/P_I$.

Among the four methods, transmission-line technique is the most widely used method. Therefore, this review mainly discusses the characterization of EMW absorption performance on the basis of the transmission line theory. The EMW absorption performance is evaluated by the reflection loss (RL),

which can be calculated by Equation (11) [126]:

$$RL = 20 \log_{10} \frac{|Z_{in} - Z_0|}{|Z_{in} + Z_0|} \quad (11)$$

where Z_{in} is the normalized input impedance of the absorber, Z_0 is the impedance of free space (and, in close approximation, of air).

$$Z_{in} = \sqrt{\frac{\mu_r}{\epsilon_r}} \tanh \left[j \frac{2\pi}{c} f \sqrt{\mu_r \epsilon_r} d \right] \quad (12)$$

where ϵ_r and μ_r are relative complex permittivity and permeability, f , c and d are frequency, the speed of EMW in free space and the thickness of the absorber, respectively.

On the basis of Equations (11) and (12), the modulus of the normalized characteristic impedance can be calculated by $Z = Z_{in}/Z_0$, representing the capability of the EMW penetrating into the absorbers and converting to other energy, such as heat energy. EMW attenuation inside the absorbers is one of the key factors for excellent EMW absorption materials, and the attenuation constant (α) is described by Equation (13) [127]:

$$\alpha = \frac{\sqrt{2\pi f}}{c} \times \sqrt{(\epsilon''\mu'' - \epsilon'\mu') + \sqrt{(\epsilon''\mu'' - \epsilon'\mu')^2 + (\epsilon''\mu'' + \epsilon'\mu')^2}} \quad (13)$$

where, ϵ' and μ' are the real part of permittivity and permeability, respectively, ϵ'' and μ'' are the imaginary part of permittivity and permeability, respectively. Apart from Z and α , EMW absorption performance can also be influenced by the thickness of the absorbers. It can be explained by a quarter-wavelength matching model, which can be expressed by the following equation [128,129]:

$$t_m = \frac{n\lambda}{4} = \frac{nc}{4f_m \sqrt{|\epsilon_r||\mu_r|}} \quad (n=1,3,5,\dots) \quad (14)$$

where λ is the wavelength in the samples, t_m is the thickness of the absorbers, and f_m is the associated frequency of the minimum RL, ϵ_r and μ_r are relative

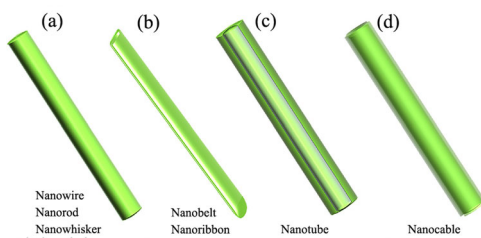


Figure 8. One dimensional SiC with various morphologies (a) nanowire, nanorod or nanowhisker; (b) nanobelt or nanoribbon; (c) nanotube and (d) nanocable (reprinted with permission of Elsevier) [21].

complex permittivity and permeability, respectively. Based on Equation (14), the best absorbent thickness and the most effective frequency range can be deduced, which is an effective method for guiding the design of excellent EMW absorbing materials.

EMW absorbing performance of dielectric-loss-type ceramics

Non-oxide ceramics

Non-oxide-based ceramics have obtained great attention as EMW absorbers in recent years due to their attractive properties such as resistance to corrosion and oxidation as well as excellent thermomechanical properties in various environments. SiC is an ideal candidate material for EMW absorption due to its adjustable dielectric properties and various morphologies (Figure 8) [21]. Li et al. investigated the effects of the annealing temperature of polymer-derived SiC on the EMW absorption performance [130]. Nano-crystals of SiC and free carbon nanodomains were gradually formed in polymer-derived SiC-based materials. Moreover, RL of the samples decreased with increasing annealing temperature, enhancing the relative complex permittivity of the materials. However, the average minimum RL (RL_{min}) of the samples obtained at 1400°C was only -9.97 dB with a sample thickness of 2.75 mm. Porous SiC nanowires (NWs) were successfully synthesized using mixtures of SiC powder with various amounts of polycarbosilane (PCS) [131]. The RL_{min} of porous SiC NWs decreased from -7.6 to -67.4 dB with increasing PCS contents, and the effective absorption bandwidth (EAB) was up to 8.1 GHz. The excellent EMW absorption performance is attributed to the formation of SiC NWs, porosity, nano-crystals and free carbon nanodomains, which result in electronic dipole polarization and interfacial polarization, due to significantly enhanced amounts of interfaces and grain boundaries as well as defects.

Si(B)CN ceramics based on SiC and Si_3N_4 provide great possibilities to tailor EMW absorbing properties of ceramics. Guo et al. measured the EMW absorption properties, complex permittivity and dielectric loss tangent of SiCN ceramics at different annealing temperatures (900–1400°C) [132]. The maximum values of ϵ' and $\tan\delta$ were 4.5 and 0.6, respectively. The RL of as-prepared sample at 1100°C was below -10 dB in a wide frequency range of 6–16 GHz (i.e. the effective band width was up to ca. 10 GHz). The degree of crystallization of free carbon was gradually improved with the increase of annealing temperature, leading to an enhancement of the dielectric loss [133]. Ye et al. investigated the EMW absorption performance of SiBCN ceramics in the frequency range of 8.2–12.4 GHz [87]. The RL_{min} and EAB of the resultant

SiBCN ceramics were -16.25 dB and 3.61 GHz, respectively, at a thickness of 2.5 mm. After annealing at elevated temperatures, nano-crystals of SiC are gradually separated from the amorphous SiBCN matrix, and the crystallization degree of free carbon increased with the increase of annealing temperature. The crystallized SiC nanocrystals and free carbon form a powerful conductive network in SiBCN ceramics, leading to increased dielectric loss and EMW absorbing performance.

Oxide ceramics

Oxide ceramics such as BaTiO_3 , Mn_2O_3 , and ZnO have also gained interest as EMW absorbing materials due to their unique chemical and physical properties. Yang et al. reported that single-crystalline ultrathin BaTiO_3 nanowires possess improved EMW absorption performance compared with BaTiO_3 nanotorus and nanotubes [91]. The nanowires exhibited a RL_{min} of -24.6 dB at 9.04 GHz and an effective absorption bandwidth of 2.4 GHz. As can be seen from Figure 9, the length (approximately several tens of micrometers) inside ultrathin nanowires plays a vital role in relaxation. Moreover, remarkable EMW absorption performance of Mn_2O_3 and Mn_3O_4 nanowires was achieved owing to an unique morphology and relatively high dielectric loss tangent [134]. The minimum RL values of Mn_2O_3 and Mn_3O_4 nanowires were -21.0 dB at 18.0 GHz and -21.2 dB at 7.7 GHz, respectively. These Mn_2O_3 and Mn_3O_4 nanowires show excellent EMW absorption properties in comparison with previously reported sponge-like Mn_2O_3 , sphere-like Mn_3O_4 nanoparticles [135], and MnO_2 nanowires [136].

In addition to the materials mentioned above, there are other ceramics that possess even better EMW absorption performance. Table 1 summarizes the EMW absorption performance of some typical dielectric-loss-type ceramics.

Ceramic (nano)composites

A detailed investigation of the properties of already existing EMW absorption materials revealed that single-component materials cannot be suitable for all EMW absorption aspects due to their relatively weak absorbing capability. Thus, more efforts have been devoted to the fabrication of composites or nanocomposites, in which single-component ceramics are combined with magnetic and/or dielectric loss materials to achieve synergistic effects on the dissipation of the EMW energy. Up to now, numbers of ceramic-based composites or nanocomposites have been proven to exhibit excellent EMW absorbing performance, such as three-dimensional (3D) RGO/ZnO composite [137], graphene nanosheet containing (GN)/ Al_2O_3

ceramics [138], nitrogen-doped graphene (N-GP)/ Ti_3C_2 nanosheets [139], RGO-SiBCN composites [140] and core-shell structured $\text{Fe}_3\text{Si}@\text{C}/\text{SiC}/\text{Fe}_3\text{O}_4/\text{SiO}_2$ nanocomposites [141].

Transition metal carbide/nitride/silicide containing ceramic (nano)composites

In recent years, transition metal carbide/nitride/silicide containing ceramic (nano)composites have attracted great interest as high-performance EMW absorbers due to their outstanding dielectric properties and highly thermal stability. The EMW absorption performance of $\text{SiC}/\text{HfC}_{x}\text{N}_{1-x}/\text{C}$ ceramic nanocomposites was investigated in the X band (8.2 – 12.4 GHz). It was found that $\text{SiC}/\text{HfC}_{x}\text{N}_{1-x}/\text{C}$ ceramic nanocomposites showed improved EMW absorption performance as compared with that of SiC/C under the same condition [142]. The enhanced EMW absorption performance is intimately connected with segregated carbon, $\text{HfC}_{x}\text{N}_{1-x}$ nanoparticles, and their special core-shell microstructure. A conductive network was formed with the help of segregated carbon between the $\text{HfC}_{x}\text{N}_{1-x}$ nanoparticles and the SiC matrix. The hafnium carbonitride nanoparticles and carbon significantly improved the electrical conductivity or imaginary part of the complex permittivity, leading to excellent EMW absorption performance. Another example relates to a $\text{Mo}_{4.8}\text{Si}_3\text{C}_{0.6}/\text{SiC}/\text{C}_{free}$ (C_{free} : free carbon) ceramic nanocomposite containing a highly conductive intermetallic Nowotny phase (NP) $\text{Mo}_{4.8}\text{Si}_3\text{C}_{0.6}$ synthesized via the polymer-derived-ceramic (PDC) approach [143]. The as-obtained ceramic nanocomposites exhibit significantly improved EMW absorption properties in comparison with well-known $\text{SiC}/\text{C}_{free}$ and $\text{MoSi}_2/\text{SiC}/\text{C}_{free}$ composites prepared under the same conditions. Besides the presence of the highly conductive intermetallic NP, the free carbon content can be tuned through the molecular design of the single-source precursors (SSP).

Nanocomposites based on $\text{ZrN}_{0.4}\text{B}_{0.6}/\text{SiC}$ with enhanced EMW absorption capability were fabricated by chemical vapour deposition (CVD) and chemical vapour infiltration (CVI) techniques. The RL_{min} reached -50.8 dB at 7.7 GHz with a thickness of 3.05 mm [65]. The excellent EMW absorbing performance is attributed to synergistic features of the $\text{ZrN}_{0.4}\text{B}_{0.6}/\text{SiC}$ nanocomposites such as reasonable conductivity of $\text{ZrN}_{0.4}\text{B}_{0.6}$, 3D networks of SiC nanofibres, and effective interface between $\text{ZrN}_{0.4}\text{B}_{0.6}$ and SiC. The performance was proven to be linked with dipole polarization, well-defined Debye relaxation, interfacial polarization and Maxwell-Wagner relaxation. Furthermore, the $\text{ZrN}_{0.4}\text{B}_{0.6}/\text{SiC}$ nanocomposites exhibited good oxidation resistance even at 600°C . Dielectric properties and EMW absorbing performance of porous carbon reinforced with Mo_2C nanocomposite were reported by Dai et al [144]. The

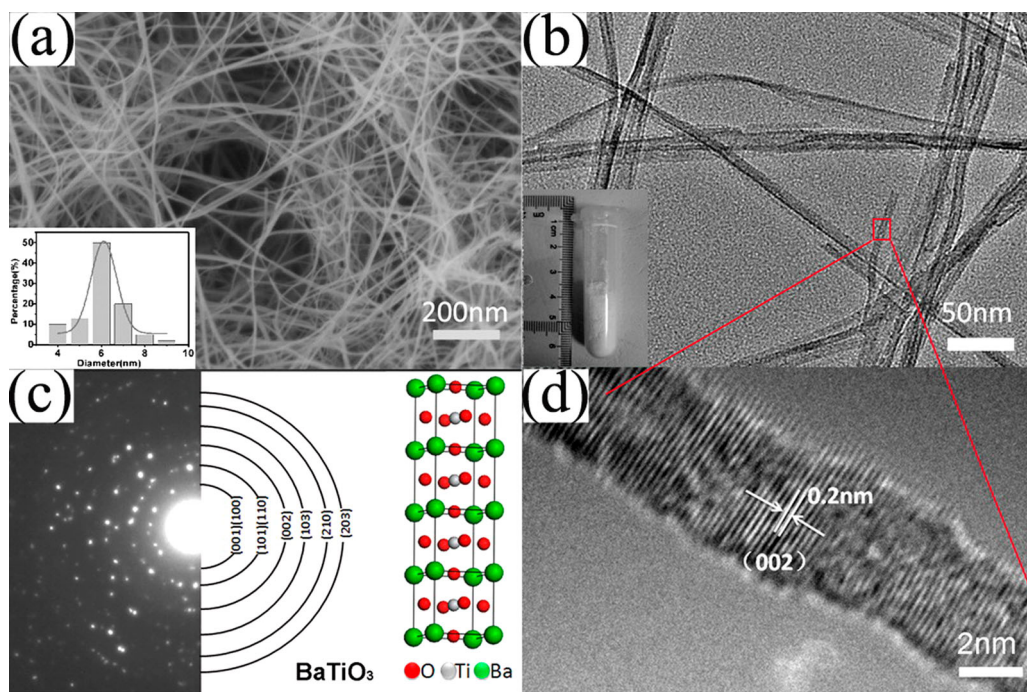


Figure 9. (a) SEM and (b) TEM micrographs of ultrathin BaTiO_3 nanowires. Inset in (a) is the diameter distribution of the BaTiO_3 nanowires. Inset in (b) is a photograph of the samples. (c) SAED pattern taken from an area containing a great amount of nanowires and (d) HRTEM image of one nanowire (reprinted with permission from American Chemical Society) [91].

as-designed Mo_2C nanocomposite not only possess enhanced impedance, but also bring about strong attenuation abilities owing to interfacial polarization derived from the large surface area and porous feature.

Carbon enhanced ceramic (nano)composites

Carbonaceous materials, such as carbon black (CB), carbon nanotubes (CNTs), graphite flakes (GFs), carbon fibres (CFs), graphene and reduced graphene oxide (RGO), have been extensively used to enhance the EMW absorbing performance of ceramic (nano)-composites because of their excellent electrical conductivity and low density [15,35,37,106,145–147]. Meanwhile, the ceramic matrix protects the carbonaceous materials from oxidation and provides strong mechanical properties.

Wan et al. designed and fabricated CB reinforced SiC fibre/aluminium phosphate matrix composite by a laminating method [148]. The real and imaginary part of the permittivity of the composites were proportional to the carbon black content, and the growth rates of the real and imaginary part of the complex permittivity showed a clear difference in terms of amount of filler. The composites with 4 wt.% CB loading exhibited outstanding effective absorption bandwidth at various matching thicknesses (2.8, 2.9, 3.0 and 3.1 mm), covering almost the entire X band.

Graphite has obtained much attention for the application in EMW absorption field due to its low cost, facile synthesis process and high electrical conductivity [149–152]. Wang et al. designed and synthesized a composite material with adjustable EMW absorbing

performance by encapsulating graphite into SiC nanowires [153]. The resultant graphite/SiC hybrid nanowires with a sample thickness of 1.7 mm exhibited a RL_{\min} of -22 dB at 16.8 GHz with the EAB covering 4.7 GHz. The improved EMW absorption performance is attributed to diverse dielectric loss mechanisms, which not only originate from the conductivity of graphite, but are also caused by interfaces between graphite and SiC, defects in graphite and SiC, as well as dangling bonds of the nanowires surface.

Carbon fibres (CFs) are suitable for EMW absorption application due to their good electrical conductivity, low density, high specific strength and large aspect ratio [147,155–157], which can significantly improve the multiple reflections with a longer propagation distance inside the composites. Li et al. reported the EMW absorption performance of magnetic Fe-Co alloy coated on CFs at 2–18 GHz frequency [158]. The as-prepared composites showed an enhanced EMW absorption, the RL_{\min} reached -48.2 dB at a coating thickness of 1.7 and RL below -10 dB covering the whole frequency range. Apart from dipoles and inductive loss, multipolar interfaces caused by the CFs and the magnetic alloy coating play a vital role. Wang et al. investigated the dielectric properties and the EMW absorption performance of the CFs/SiC nanofibre composites at the frequency range of 2–18 GHz by tuning the weight ratio of the precursors [154]. The CFs/SiC nanofibre composites displayed an excellent EMW performance, the optimal RL reached values as high as -57.8 dB at a coating thickness of 1.9 mm. In addition, the carbon nanofibre reinforced CFs/SiC

Table 1. EMW absorption performance of ceramic (nano)composites (CIP: carbonyl-iron powder; GNSs: graphene nanosheets; PyC: pyrolytic carbon; CNFs: carbon nanofibres; real part (ϵ') and imaginary part (ϵ'') permittivity are approximate values estimated from the cited literatures).

Materials	Thickness (mm)	Frequency (GHz)	RL (dB)	EAB (GHz)	Complex permittivity		Weight per cent (%)	Matrix	Ref.
					Real part (ϵ')	Imaginary part (ϵ'')			
SiOC	2.95	10.11	-58.4	X band	3.94–9.14	2.27–4.13	100	~	[174]
SiC	3.8	9.60	-26.7	3.1	2.18–4.56	1.88–2.56	~	paraffin	[175]
Bulk SiOC	2.2	15.76	-15.8	Ku band	3.71–4.06	2.03–2.49	100	~	[176]
Mn ₂ O ₃	2.0	18.0	-21.0	~	3.89–8.00	1.73–5.00	50	paraffin	[134]
MnO ₂	4.0	5.30	-18.4	1.4	10.00–14.00	2.00–5.00	75	paraffin	[136]
Ti ₃ SiC ₂	2.0	9.73	-33.8	X band	10.92–16.11	2.13–7.13	~	paraffin	[94]
ZnO	4.0	4.2	-58.0	~	5.00–6.50	1.00–1.50	60	paraffin	[177]
SiCN	3.35	~	-53.0	3.0	5.71–5.99	2.76–3.15	100	~	[178]
Mn ₃ O ₄	5.00	7.70	-21.2	4.4	4.03–14.51	2.69–10.78	50	paraffin	[134]
BCN	4.5	5.44	-52.7	~	6.32–12.43	2.17–5.83	16.7	paraffin	[179]
TiCN	1.88	13.20	-29.1	5.4	7.53–10.39	3.09–6.11	28.6	paraffin	[115]
SiCNWs	2.0	8.3	-31.7	2.5	5.39–12.61	-0.73–2.00	35	epoxy	[60]
SiC fibres	4.7	8.2	-30.0	2.6	2.23–4.59	1.64–2.37	55	epoxy	[180]
TiC	5.0	13.8	-16.1	1.7	10.41–14.37	0.52–4.51	30	paraffin	[181]
SiCNWs	3	11.2	-17.4	2.5	3.83–8.07	-1.00–3.86	30	~	[182]
graphite/SiC	1.7	16.8	-22.0	4.7	7.35–10.31	1.73–2.79	35	paraffin	[153]
graphite/SiC/Si ₃ N ₄	2.5	17.1	-32.3	6.4	4.52–9.34	2.11–3.05	16.6	paraffin	[183]
CIP/CB	1.5	15.9	-17.5	~	25.01–38.65	8.26–18.42	45	epoxy	[184]
CB/SiC	2.0	9.0	-41.0	6.0	~	~	55	paraffin	[185]
1D carbon/SiC	1.9	5.5	-57.8	5.5	7.29–12.64	3.12–3.76	35	paraffin	[154]
RGO/SiO ₂	3.3	~	-36.0	X band	3.78–4.72	2.46–3.31	100	~	[186]
RGO/ZnO	4.8	9.57	-27.8	X band	3.04–3.41	1.52–2.13	100	~	[187]
CFs/SiO ₂	5.0	9.9	-10.2	~	24.43	11.51	100	~	[188]
CNTs/SiC	3.35	14.5	-37.6	1.5	6.25–7.45	0.89–1.39	20	paraffin	[189]
CNT@TiO ₂	2.0	10.35	-31.8	2.8	11.09–14.87	3.21–5.67	30	paraffin	[190]
GNSs/MgO	1.5	10.7	-36.5	3.0	21.82–25.33	2.56–5.61	100	~	[191]
CNT/SiCNW	2.5	10.01	-33.8	3.4	8.37–15.63	3.27–4.29	30	paraffin	[192]
SiCNWs/PyC-SiC _x /SiC	2.2	15.6	-58.5	6.1	4.91–6.53	0.97–3.62	30	paraffin	[193]
C _{free} /SiCN	2.2	2.7	-17.8	~	11.42–12.95	5.67–5.96	100	~	[194]
graphene/SiBCN	2.0	15.5	-21.0	4.7	5.73–8.99	2.23–3.78	~	paraffin	[195]
MWCNTs/SiC/SiOC	2.19	~	-61.8	2.6	13.23–13.65	4.25–4.43	~	paraffin	[196]
CNFs/SiOC	2.3	12.24	-47.9	4.6	7.02–11.83	2.96–4.12	50	paraffin	[197]
C/B ₄ C	1.5	15.5	-60.8	~	11.52–18.78	4.21–7.49	60	paraffin	[198]
rGO/h-BN	1.6	15.3	-40.5	5.0	7.67–14.86	0.59–7.43	25	paraffin	[199]
Fe ₃ Si/SiC@SiO ₂	4.9	15.5	-37.5	6.0	5.18–11.29	-1.96–4.32	30	paraffin	[200]

composites exhibited a strong EMW absorption capability with an ultra-wide EAB covering half of the X band and the whole Ku band. As can be seen from Figure 10, the outstanding EMW performance of the CFs/SiC composites is attributed to SiC nanocrystals, defects of carbon, interfaces, high aspect ratio of CFs/SiC nanofibres and their synergistic effects.

CNTs with adjustable conductivity have been widely used as EMW absorption materials [159–162].

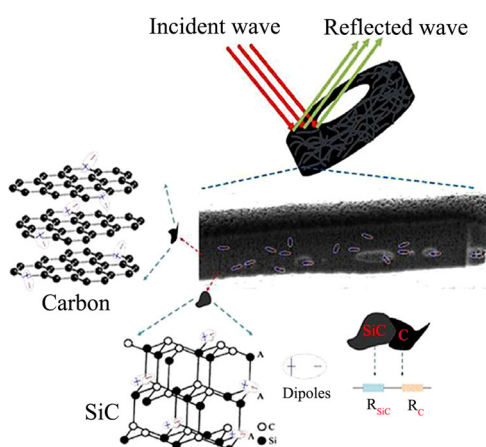


Figure 10. Schematic diagram for EMW loss mechanism of nanofibres (reprinted with permission of Elsevier) [154].

However, the application of CNTs as EMW absorbers in ceramic composites was limited because of the difficulty in uniform dispersion of CNTs in the ceramic matrix. Therefore, the preparation of CNTs/ceramic (nano)composites with homogeneously dispersed CNTs has become a research hotspot in recent years. For instance, CNTs/SiOC composites were prepared by the PDC route using unfunctionalized and functionalized CNTs and polysiloxane (PSO) as the precursor to form the ceramic matrix [163].

CNTs/SiOC composites containing 7.5 wt.% of carboxyl-modified CNTs (CNTs-COOH) exhibited much better mechanical properties and EMW absorption performance than CNTs/SiOC with hydroxylated CNTs (CNTs-OH) and pristine CNTs. These results attribute to the homogeneous dispersion of CNTs-COOH in PSO/ethanol solution due to stronger electrostatic repulsions with each other and strong binding forces with PSO. Wei et al. reported the EMW absorption performance of CNTs/Sc₂Si₂O₇ ceramic composites prepared by CVD technology [164]. The CNTs/Sc₂Si₂O₇ composite loaded with 1.56 wt.% CNTs exhibited an excellent EMW absorbing performance with minimal RL peak of -33.5 dB at the thickness of 2.85 mm, and the EAB covered the

whole X band (4.2 GHz). In addition to large amounts of interfaces formed on the porous $\text{Sc}_2\text{Si}_2\text{O}_7$ matrix due to the coils of CNTs, the defect concentrations of CNTs/ $\text{Sc}_2\text{Si}_2\text{O}_7$ composite can be optimized, which are helpful for the multiple reflection and dissipation of the EMWs. Another example is related to CNT/SiC_f composites which were successfully synthesized with a new developed method using ferrocene as both carbon source and catalyst (Figure 11) [165]. As can be seen from Figure 11, the CNT/SiC_f composites (with CNT content of 0.72 wt.%) were proven to possess outstanding EMW absorbing performance with RL_{\min} of -62.5 dB and EAB of 8.8 GHz which covered almost the entire Ku-band and three-quarters of X-band. Moreover, the EMW absorption performance and other properties of the composites can be modified by adding to various different materials. Furthermore, a MWCNTs/Al₂O₃ composite containing 3.8 wt.% chopped multi-walled carbon nanotubes (MWCNTs) showed an enhanced EMW absorption performance with RL_{\min} of -37 dB and the EAB of 2.5 GHz, which is much better than that of pristine materials without MWCNT fillers [166].

Compared with CNTs, graphene exhibits superior chemical and physical properties due to the unique two-dimensional structure, such as high carrier mobility, excellent electrical conductivity, large specific surface area, high specific strength and low density [167–172]. Therefore, graphene reinforced ceramic composites are now standing at the frontier of high-performance EMW absorption materials. Most importantly, the graphene enhanced ceramic composite/nanocomposites have great potential to overcome the challenges related to the integrated structural and functional requirements of the EMW absorbing materials.

A CVD route for the direct growth of edge-rich graphene (ERG) in porous Si₃N₄ ceramics with tailoring structures and tunable dielectric properties was reported in reference [71]. The unique microstructure of the as-prepared ERG/Si₃N₄ composites (i.e. containing open graphite nanosteps and freestanding nanoplates) provide an appropriate balance between good impedance matching and strong dielectric loss capacity. Taking advantage of the synergistic effect of insulating Si₃N₄ and highly conductive graphene as well as of the special tremendous ‘resistance-inductance-capacitance’ coupled circuit structures, the ERG/Si₃N₄ composites exhibited superior EMW absorption performance with EAB covering the whole X band at a thickness of 3.75 mm with a negligibly loading content of absorbers. In Liu et al.’s work [173], the RGO/SiCN composites prepared by single-source-precursor (SSP) approach and mechanical blending method exhibited a significant difference in EMW absorption performance. The disadvantages caused by restacking of graphene oxide (GO) are effectively prevented via chemical modification of GO with

poly(methylvinyl)silazane. Accordingly, the RGO/SiCN composite with 2.5 wt.% GO in feed exhibited outstanding EMW absorbing performance with RL_{\min} of -62.1 dB at 9.0 GHz at the thickness of 2.1 mm. With the same GO in feed, the RL_{\min} of RGO/SiCN composite prepared by mechanical blending was only -8.2 dB. The huge difference in the minimal RL_{\min} of the samples prepared by SSP approach and mechanical blending method can be explained by the quality of the dispersion of RGO in the ceramic matrix, as shown in Figure 12. Various carbon enhanced ceramic (nano)composites used for EMW absorbing applications are summarized in Table 1.

EMW absorbing performance of magnetic-loss-type ceramics

Magnetic metal particles (e.g. Fe, Co, Ni) and their related chemical compounds (e.g. Fe₃Si, Fe₂O₃, Fe₃O₄, NiO, Co₃O₄, Fe₃C, CoFe₂O₄) not only have large saturation magnetization, high Snoek’s limit, and distinguishable permeability, but also possess good compatible dielectric loss in the gigahertz frequency range. Therefore, magnetic metal and their compounds attract much attention because they can meet the feature requirements for high-performance EMW absorption materials [156,201–207]. However, poor mechanical strength and corrosion resistance limit their widespread applications. Therefore, incorporation of magnetic materials into a ceramic matrix is a good strategy to prepare EMW absorbing materials with excellent mechanical properties and corrosion resistance. Consequently, in recent years, a large number of magnetic metals related to ceramic composites with outstanding EMW absorption performance have been studied [64,78,208–213].

Iron containing ceramic composites

As typical magnetic materials, Fe-containing compounds have been taken as one of the most commonly used fillers in ceramic-based EMW absorption materials. For instance, Hou et al. decorated amorphous SiOC ceramics with carbon-coated Fe₃Si nanoparticles (SiOC/C/Fe₃Si). They found that the resultant composites exhibited much better RL characteristics than any two-component materials by adjusting the magnetic components [214]. The SiOC/C/Fe₃Si composites loaded with 12.33 wt.% Fe (thickness: 3.5 mm) possessed a minimal RL of -41 dB at 7.9 GHz, and the EAB covered the whole S band (2–3.95 GHz). Hou et al. reported the synthesis of Fe/SiC hybrid fibres by electrospinning method using PCS and Fe₃O₄ precursors, as shown in Figure 13 [67]. The study showed that the introduction of Fe had a dramatic impact on the morphology and EMW absorbing performance of the SiC hybrid

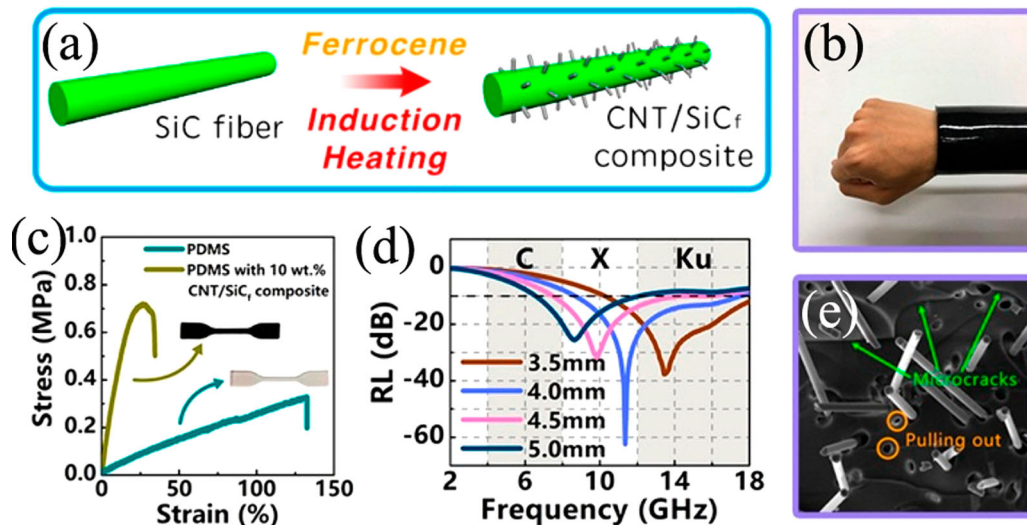


Figure 11. (a) Schematic illustration of the preparation process of CNT/SiC_f composite; (b) Photo of a composite made of poly-dimethylsiloxane (PDMS) mixed with CNT/SiC_f; (c) Stress-strain curves of pure PDMS and composite with 10 wt.% CNT/SiC_f; (d) RL of CNT/SiC_f composite with 0.72 wt.% CNT; (e) SEM image of the fractured surface of PDMS with 10 wt.% CNT/SiC_f (reprinted with permission from American Chemical Society) [165].

fibres. The as-prepared Fe/SiC fibre composites were found to be a characteristic dielectric/magnetic medium with multiple loss mechanisms such as magnetic loss from Fe, dielectric loss from Fe/SiC, and polarization relaxation loss from the hybrid interface.

Lou et al. pioneered the synthesis of porous 3D Fe-based/C composites such as Fe₃O₄@C, Fe₃O₄/Fe@C, and Fe₃C@C by carbonizing iron (III) 2,4-pentanedionate (Fe(acac)₃) pre-enriched forestry waste wood [215]. The resultant porous 3D Fe-based/C

composites displayed significantly improved EMW absorption properties, where the optimal RL reached -57.64 dB at 6.92 GHz, and a broad EAB of 5.0 GHz. The outstanding EMW absorption performance is attributed to continuous Fe₃C coating on the inner surface of carbon, leading to optimal impedance matching. More importantly, defects are generated in porous 3D Fe-based/C composites, which play a vital role in dipole relaxation polarization. Liu et al. successfully fabricated double-loss Ti₃SiC₂/Co₃Fe₇

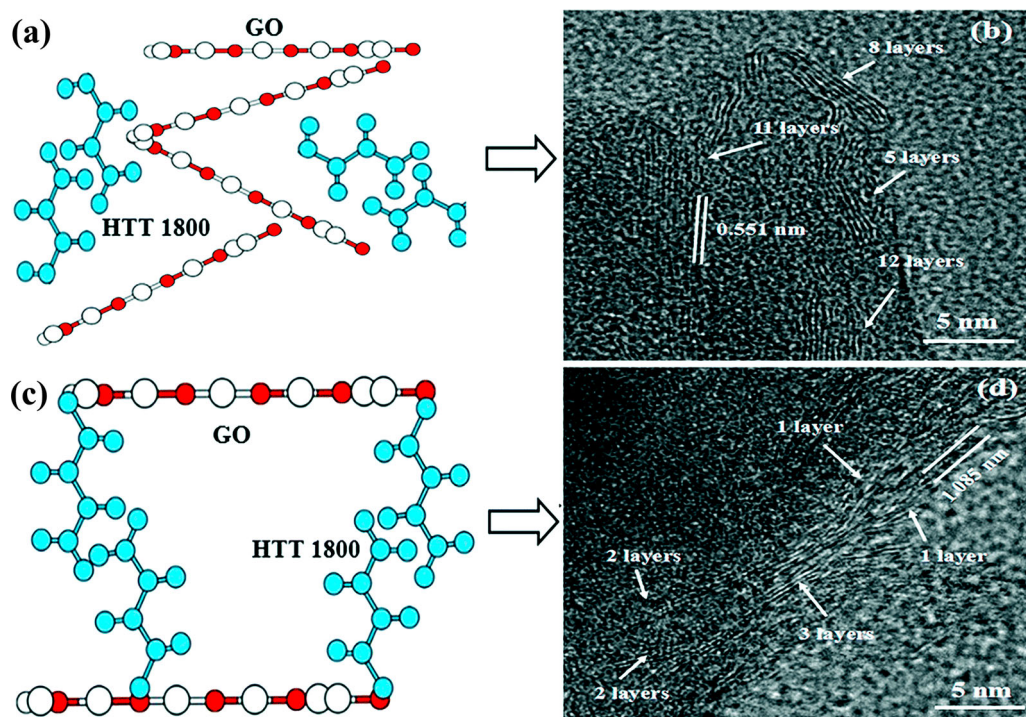


Figure 12. Schemes of (a) physically-blended-precursor (PBP) and (c) GO-containing single-source-precursor (SSP). TEM images of RGO/SiCN ceramic composites derived from (b) PBP and from (d) SSP (reprinted with permission from the Royal Society of Chemistry)[173].

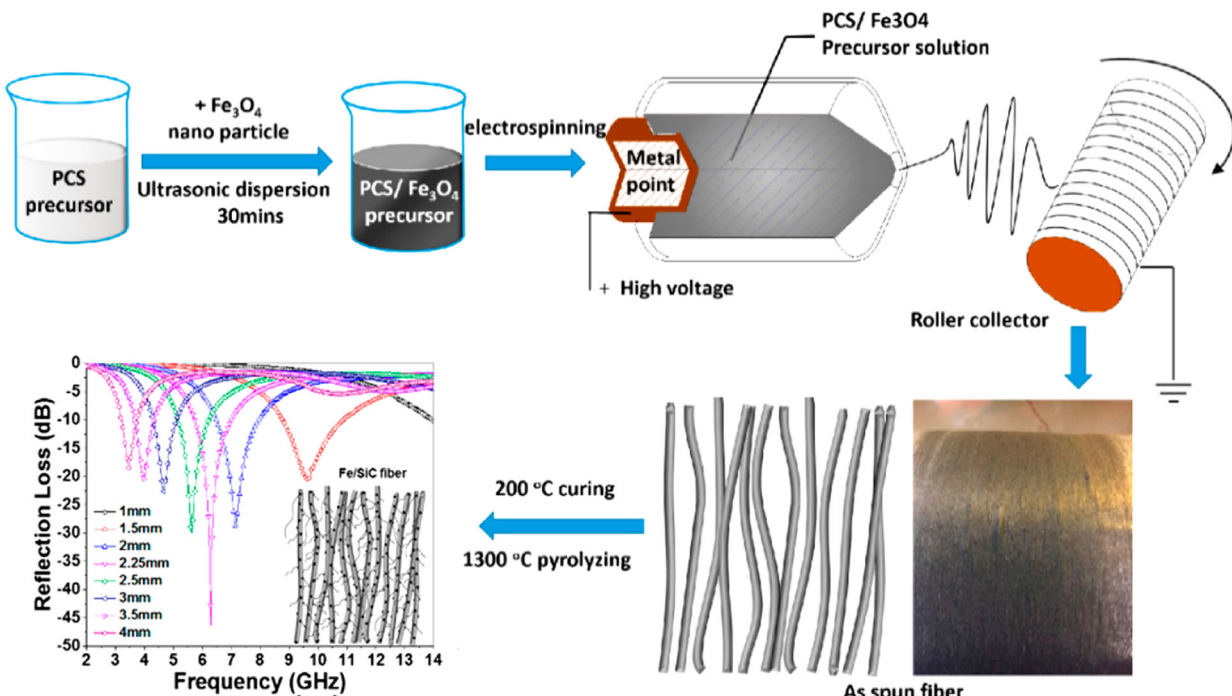


Figure 13. Schematic diagram of the preparation and RL of Fe-based/SiC hybrid fibres. The inset digital photo showed the fibres on a roller collector of the needleless electrospinning setup (reprinted with permission from American Chemical Society) [67].

composites via carbothermic reduction method [95]. The scattering of Co_3Fe_7 particles on the surface of Ti_3SiC_2 resulted in excellent EMW absorption properties, which are ascribed to an improved dielectric relaxation of Co_3Fe_7 particles and to a stronger dissipation ability of the $\text{Ti}_3\text{SiC}_2/\text{Co}_3\text{Fe}_7$ composites.

Other magnetic metals containing ceramic composites

In addition to iron-containing materials, other magnetic metals and metal compounds (e.g. Co, Ni, NiO , Co_3O_4 , etc.) have also been widely introduced into a ceramic matrix to improve the EMW absorption performance of the associated composites. For example, Luo et al. prepared cobalt-containing (Co , CoSi , Co_2Si) ceramics with high-temperature resistance by the PDC method (Figure 14) [216]. The introduction of cobalt caused an enhanced EMW absorption performance. The RL_{\min} of the sample with 3.84 wt.% Co amounted -42.43 dB at 10.55 GHz, and the EAB covered nearly the whole X-band between 8.46 and 12.4 GHz (Figure 14(d)). The excellent EMW absorption performance was confirmed to be linked to the formation of cobalt silicide nanocrystals and crystallized free carbon, which result in synergistic effects of dielectric and magnetic loss.

Ma et al. coated a layer of Ni–Co–P on the surface of SiO_2 particles. The EMW absorption analysis showed that the Ni–Co–P-coated SiO_2 was a good candidate for EMW absorption application [217]. The minimum RL reached -48.6 dB at 4.2 GHz with a thickness of 3.10 mm, which is attributed to the

optimal magnetic loss and well-matched characteristic impedance.

Huang et al. reported an EMW absorption material with bead-like Co nanoparticles embedded in a ZnO matrix, which exhibited wider EAB (6.4–18 GHz) than that of pristine ZnO and Co particles [218]. The results confirm that the presence of Co particles is responsible for the improved EMW absorption performance. The hysteresis loss and residual loss of Co particles lead to significant magnetic loss. The incorporation of Co particles results in more defects, interfacial polarization and dipole polarization due to lattice shrinkage. Furthermore, Wang et al. prepared cobalt-containing SiCN composites via the PDC route. The prepared composites exhibited stronger EMW absorption performance owing to well-matched characteristics between the dielectric property of the SiCN ceramic matrix and the good magnetic property of Co particles [219].

In addition to the aforementioned magnetic materials, manyfold other magnetic-loss-type ceramic composites with excellent EMW absorption performance are reported in the literature. Some typical magnetic-loss-type EMW absorbing ceramic composites are summarized in Table 2.

EMW absorbing performance of multinary absorbers

Recently, a large number of publications deal with the synthesis of multinary ceramic composites as high-performance EMW absorption materials. Table 3 summarizes the EMW absorption properties of some

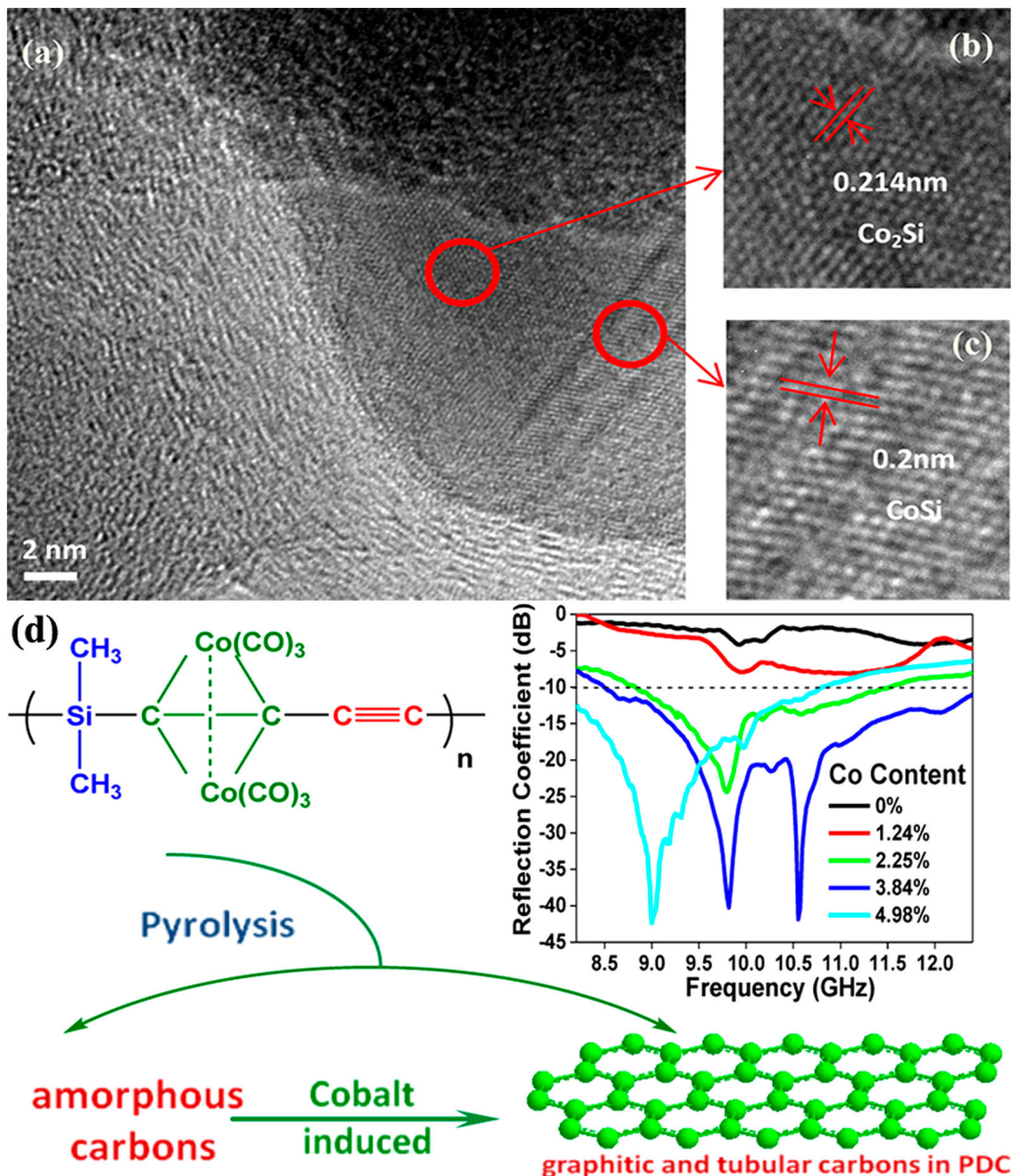


Figure 14. (a) TEM images and (b, c) high-resolution TEM images of ceramics loaded with 3.84 wt.% Co, (d) Schematic diagram of the preparation route and reflection coefficient vs frequency of the composites with varying Co-contents [216].

multinary ceramic composites. For instance, core-shell structured $\text{Fe}_3\text{Si}@/\text{C}/\text{SiC}/\text{Fe}_3\text{O}_4/\text{SiO}_2$ ceramic nanocomposites were successfully synthesized via the

PDC method. The as-fabricated $\text{Fe}_3\text{Si}@/\text{C}/\text{SiC}/\text{Fe}_3\text{O}_4/\text{SiO}_2$ composites showed significantly enhanced EMW absorbing performance, in which the optimal

Table 2. EMW absorption performance of magnetic-loss-type ceramic composites (real part (ϵ') and imaginary part (ϵ'') permittivity are approximate values estimated from the cited literatures).

Materials	Thickness (mm)	Frequency (GHz)	RL (dB)	EAB (GHz)	Complex permittivity		Weight per cent (%)	Matrix	Ref.
					Real part (ϵ')	Imaginary part (ϵ'')			
Co/SiCNWs	3.0	14.2	-25.0	6.6	4.83–5.31	1.02–1.79	50	paraffin	[220]
$\text{Fe}_3\text{O}_4/\text{SiCNWs}$	3.0	8.6	-51.0	7.0	4.66–5.92	2.73–4.22	50	paraffin	[221]
ZnO/SiCNWs	3.5	9.16	-42.1	4.5	4.74–9.26	2.17–3.84	30	paraffin	[222]
Fe/SiC whiskers	2.0	10.0	-21.0	2.6	6.52–6.54	0.26–4.18	20	paraffin	[223]
Ni/SiC	3.5	8.4	-31.0	3.4	11.81–18.29	5.54–5.07	80	epoxy	[224]
$\text{Ni}_{0.01}\text{Si}_{0.99}\text{C}$	2.8	8.8	-11.1	1.1	8.34–8.51	1.76–1.97	20	paraffin	[225]
Ag@SiC	2.0	4.66	-41.6	4.7	7.16–12.20	1.71–4.38	50	paraffin	[226]
Ni/SiCN	2.0	15.1	-48.5	0.6	0.37–9.04	0.07–6.83	~	paraffin	[227]
Fe/SiOC	4.55	5.40	-59.6	2.0	4.56–9.57	2.11–5.46	100	~	[228]
$\text{Mn}_{0.01}\text{Si}_{0.99}\text{C}$	2.8	11.1	-16.8	3.1	6.83–6.98	1.33–1.54	20	paraffin	[225]
$\text{Ni/Ti}_3\text{SiC}_2$	2.2	9.7	-41.2	3.8	15.21–22.46	4.72–10.07	~	epoxy	[229]
$\text{Al/Ti}_3\text{SiC}_2$	2.6	12.2	-16.2	4.2	6.63–10.41	4.47–7.49	50	paraffin	[230]
Fe@SiO_2	2.81	9.3	-61.6	~	7.61–8.39	2.80–2.86	50	paraffin	[231]
$\text{BCN/Fe}_x(\text{B/C/N})_y$	2.0	11.44	-47.9	~	5.25–14.86	0.04–7.67	25	paraffin	[100]

Table 3. EMW absorption performance of multinary ceramic composites (real part (ϵ') and imaginary part (ϵ'') permittivity are approximate values estimated from the cited literatures).

Materials	Thickness (mm)	Frequency (GHz)	RL (dB)	EAB (GHz)	Complex permittivity		Weight per cent (%)	Matrix	Ref.
					Real part (ϵ')	Imaginary part (ϵ'')			
C/SiC/Si ₃ N ₄	2.5	5.5	-57.8	6.4	7.12–12.07	3.24–4.22	35	paraffin	[183]
3D CNTs/Fe ₃ O ₄	6.8	12.8	-52.8	5.0	2.80–12.00	0.02–5.06	20	paraffin	[237]
Graphene@Fe ₃ O ₄ @SiO ₂ @NiO	1.8	15.76	-51.5	5.1	7.91–15.84	1.09–9.97	25	paraffin	[238]
Fe ₃ O ₄ @ZnO/RGO	5.0	~	-37.0	1.0	~	~	30	epoxy	[239]
RGO@Fe ₃ O ₄ @C@polyaniline	3.0	11.4	-44.2	5.8	5.68–11.73	0.67–6.94	25	paraffin	[240]
Ni/SiC/Graphene	1.9	15.28	-59.2	4.5	4.21–5.67	0.04–2.47	~	~	[241]
Ni(Co/Zn/Cu)Fe ₂ O ₄ /SiC@SiO ₂	3.0	6.08	-32.3	2.1	~	~	20	paraffin	[242]
Ni _{0.5} Zn _{0.5} Fe ₂ O ₄ /Ti ₃ SiC ₂	1.2	13.2	-38.6	5.3	12.66–20.08	0.09–3.59	100	~	[243]
SiC@SiO ₂ @Fe ₃ O ₄	2.0	12.24	-39.6	3.7	10.08–15.83	3.81–4.67	50	paraffin	[234]
Ti/Ni/C	1.7	12.4	-35.1	3.6	12.04–17.13	4.42–6.03	50	paraffin	[244]
h-BN/GO/Fe ₃ O ₄	2.0	5.5	-58.0	14.4	8.76–10.97	0.63–1.38	90	paraffin	[245]
Ti ₃ SiC ₂ /Cu/epoxy	2.2	10.13	-31.7	2.2	9.48–13.26	0.01–5.07	100	~	[246]
Al-doped ZnO/ZrSiO ₄	3.5	9.2	-32.0	3.6	5.14–6.28	2.61–2.94	100	~	[247]

RL reached -44.7 dB at 4.25 GHz. The EAB was up to 9.5 GHz (2.5–12.0 GHz) by tuning the sample thickness [141]. The multinary absorbers can not only manifest the magnetic loss derived from magnetic absorbers, but also generate typical dielectric loss from the presence of conductive phases. Moreover, the special interfaces formed between multinary absorbers also cause interfacial polarization and dipole polarization effects. Hou et al. fabricated high-temperature anti-oxidative SiC/Fe₃Si/CNTs ternary composites from a Fe-containing polysilyacetylene (PSA) via a one-step PDC approach (Figure 15) [232]. The RL_{min} of the SiC/Fe₃Si/CNTs composite with a thickness of 2 mm was up to -41.2 dB at 10.5 GHz, and a broad EAB (12.9–16.9 GHz) was achieved at the thickness of ca.1.5 mm. The excellent EMW absorption performance of SiC/Fe₃Si/CNTs composites is attributed to the joint effects of dielectric loss, magnetic loss, and special morphologies, which result from micron-sized SiC ceramics with spherical Fe₃Si nanoparticles and CNTs attached. In addition, ternary graphene@ polyaniline@TiO₂ [233], SiC@SiO₂@Fe₃O₄ [234], quaternary graphene@Fe₃O₄@SiO₂@ polyaniline [235] and graphene/Fe₃O₄@Fe/ZnO [236], and multinary Fe₃Si@C/SiC/Fe₃O₄/SiO₂ composites [141] were also reported.

EMW absorbing performance based on microstructural design

In addition to dielectric and magnetic properties as well as impedance matching, the EMW absorption performance of materials is closely related to their particular microstructure and morphologies of the participating phases [248–254]. These features can make incident EMW generate multiple reflections, scattering and refraction as much as possible to prolong the transmission path, which is beneficial for dissipating EM energy [251, 255–257]. Moreover, some special morphologies and structures can lead to

increase interface, leading to the effective attenuation of EMWs by space charge polarization and interfacial polarization [258–260]. In addition, as shown in Figure 6, the incident EMW is divided into four parts when it enters a material. As for some particular morphologies and microstructures of materials, destructive amplitude phenomenon will occur while the wave path difference between the absorbed EMW and the reflected EMW is an odd multiple of half wavelengths [261–263]. Furthermore, it can also make the two-wave interference and reverse the phase of the absorbed EMW and the reflected EMW to partly counteract EMW [264–270]. Therefore, it is meaningful to investigate the relationship between morphology/microstructure and EMW absorbing performance.

Dimensional effects

Numerous studies confirm that the particle size of the EMW absorbing components has a significant effect on their absorption performance [271–276]. Therefore, controlling the particle size is an effective way to tune the EMW absorption performance. For example, Wu et al. fabricated carbon-coated nickel (Ni/C) nano-capsules with the average particle size varying from 25 to 53 nm. They investigated the influence of the particle size on the magnetic properties and associated EMW absorption performance [273]. They found that the saturation magnetization increases with increasing particle size, however, the complex permittivity, dielectric loss and attenuation constant of Ni/C composites increase with decreasing particle size of Ni/C nano-capsules. This behaviour is attributed to the larger specific interface area and higher number of defects associated with the smaller nano-capsules. In another case, Co₇Fe₃ and Co₇Fe₃@SiO₂ nanospheres with diameters from 350 to 650 nm were synthesized for high-performance EMW absorption application [277]. Compared with Co₇Fe₃

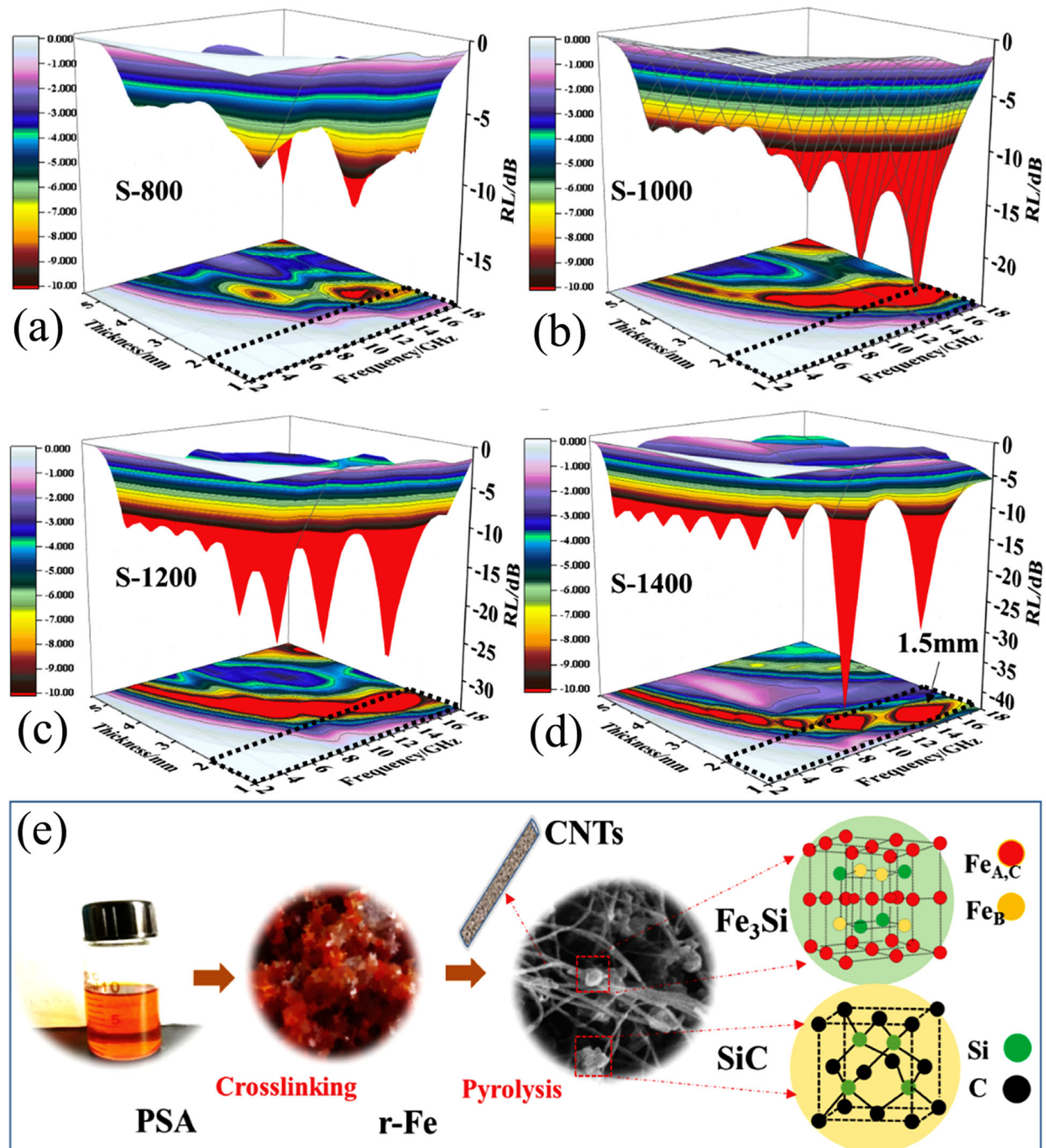


Figure 15. Three-dimensional reflection loss (in dB) patterns of the SiC/Fe₃Si/CNTs composites obtained at: (a) 800°C; (b) 1000°C; (c) 1200°C and (d) 1400°C; (e) fabrication process of the SiC/Fe₃Si/CNTs composites [232].

with a diameter of 650 nm, the optimal RL value of the nanospheres was obtained with a diameter of 350 nm, namely -78.4 dB at a thickness of 1.59 mm. As shown in Figure 16, the smaller size of the spheres is helpful to increase the saturation magnetization [272], which results in an increase of the permeability and enhancement of the magnetic loss.

Multilayered gradient ceramics

In order to further promote the EMW absorption performance, particularly to extend the EAB, multilayer absorbing materials have been developed in recent

years. Multilayered gradient ceramics consist of multi-components with magnetic and dielectric properties, resulting in various dissipative mechanisms. Furthermore, the special interface in multilayer absorbers is able to cause interfacial polarization and dipole polarization. Figure 17 shows the schematic illustration of a nine-layer absorbing material. One example is a multilayered gradient epoxy-matrix composite comprised of carbon nanotubes, silicon carbide and carbonyl iron particles, fabricated by a powder spraying method [278]. However, the results displayed that the RL_{min} of the multilayered composites was only -17.8 dB. Chen et al. prepared a multilayered CNTs/

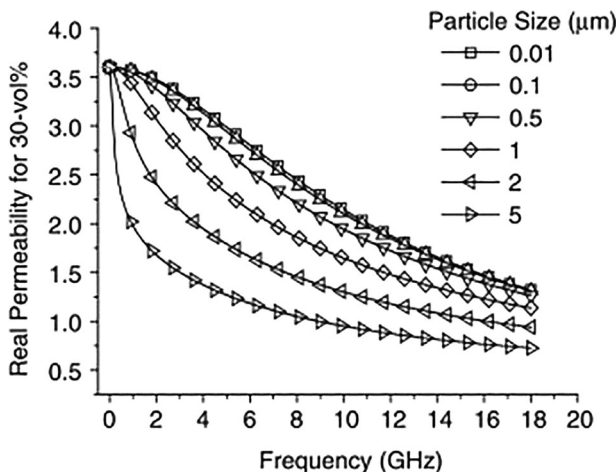


Figure 16. The influence of the particle size on the real permeability in Fe/epoxy resin (reprinted with permission of Elsevier) [272].

silicon dioxide composite (denoted as CNTs/SiO₂) by using hot-pressing for sintering. The gradient CNTs/SiO₂ composite was constructed by adding five layers of mixed powders with different CNT contents (0, 2.5, 5, 7.5 and 10 wt.%). The resultant CNTs/SiO₂ composites exhibit 1.5 times of the EMW absorption capability than that of the traditional CNT/SiO₂ composite [80]. Moreover, pyrolytic carbon-Si₃N₄ ceramic composites with gradient PyC distribution (Gradient-PyC-Si₃N₄) were prepared by directional oxidation PyC-Si₃N₄ in the air with the help of Si₃N₄ coating. After oxidation for 1.0 h, the EMW absorption ability of the Gradient-PyC-Si₃N₄ increased from 0.8 to 50.1% [279].

Special morphology and microstructure

In recent years, core-shell structured ceramic composites are elaborately prepared to remedy the shortcomings in conventional ceramic composites. As shown in Figure 18, core-shell type Ni@SiC composites with an outstanding chemical homogeneity were synthesized [280]. The synergistic effect between the SiC coating and Ni nanoparticles provides an enhanced EMW absorption performance, where the RL_{min} of the core-shell Ni@SiC composites achieved -42.1 dB at 11.2 GHz, and the EAB covered the entire X-band at a thickness of 2.88 mm. Moreover, the as-fabricated core-shell Ni@SiC composites exhibit much better EMW absorption performance than that of Ni particles embedded in a SiC matrix [241]. The experimental results indicate that the excellent EMW absorption performance of the core-shell Ni@SiC composites is owing to a good impedance matching as well as to the increased relaxation and interfacial polarization arising from the core-shell structure.

Zhou et al. prepared a series of hierarchical CoNi@SiO₂@C composites. The urchin-like CoNi

alloy particles were successfully encapsulated with SiO₂ and carbon coatings [281]. The as-prepared CoNi@SiO₂@C composites produced stronger EMW absorption with different absorber thicknesses. The excellent EMW absorption performance is caused by a combination of dielectric and magnetic loss. The complicated interfacial polarization and dipolar polarization phenomena are explained by their hierarchically multi-component structure.

In another case, a novel worm-like SiC/B₄C composite was successfully fabricated via a multi-step vapour-liquid-solid process (Figure 19) [282]. The resultant SiC/B₄C composite showed an EAB up to 4.9 GHz (7.4–12.3 GHz) at 3.7 mm, which covered the entire X-band. Moreover, the minimal RL reached to -50.81 dB at 11.9 GHz with the thickness of 3.3 mm, which is almost three times higher than that of B₄C nanowires. The excellent EMW absorption capability is mainly derived from the abundant defects and improved double dielectric relaxation, including interfacial polarization and electric dipole polarization.

Wang et al. successfully designed and prepared a tremella-like graphene@SiC core-shell nano-structure composite with a great potential in the EMW absorption application [283]. The significantly enhanced EMW absorption performance is considered to be associated with its special structural characteristics (tremella-like surface and core-shell structure), which strongly affects the characteristic impedance (conductive graphene and semiconducting SiC) and their multiple polarization. Even more EMW absorbing materials with unique morphologies and microstructures, such as dual-shells, hollow microspheres, flower-like and bone-like structures, etc. are listed in Table 4.

High-temperature EMW absorbing performance

The EMW absorption materials applied in harsh environments such as high temperature (> 600°C) and oxidative atmosphere are highly desired for high precision electronic devices, aircraft engine nozzles or their aerodynamically heated parts. Conductive polymers, magnetic metals and some carbonaceous materials exhibit good EMW absorption at room temperature. Nevertheless, EMW absorbing applications of polymers at elevated temperatures are limited by their rather low melting/softening/decomposition points (< 300°C). Magnetic-loss-type materials also lose their superiority when the temperature is higher than the Curie point. Carbonaceous materials exhibit poor oxidation resistance at temperatures higher than 350°C. Therefore, dielectric-loss-type ceramic-based materials are generally regarded as a promising candidate for EMW absorption at high temperatures.

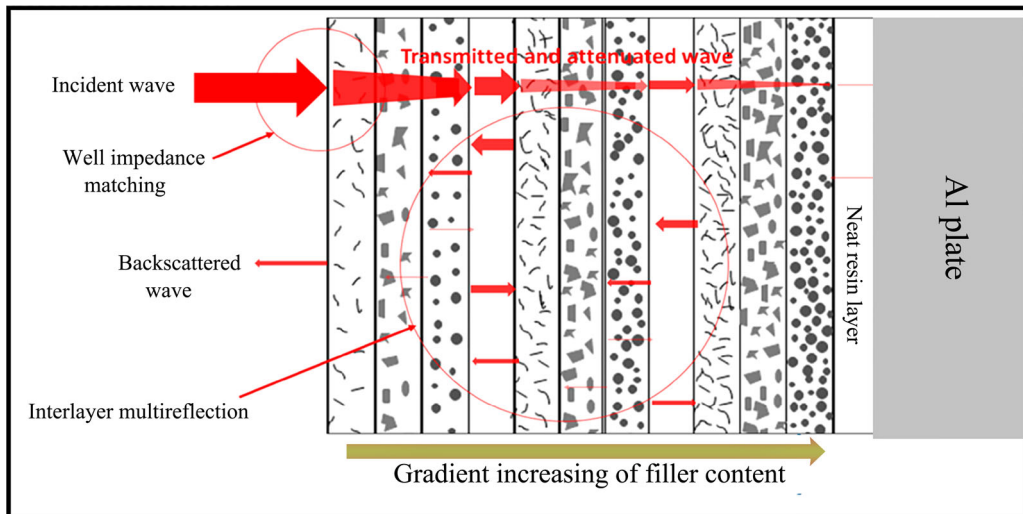


Figure 17. Schematic illustration of a multilayered EMW materials structure. The nine single-layer gradient structure is composed of epoxy resin and fillers with different weight ratios, the fillers from left to right are 3 wt.% CNT, 5 wt.% CNT, 7 wt.% CNT, 30 wt.% SiC, 40 wt.% SiC, 50 wt.% SiC, 60 wt.% carbonyl iron, 70 wt.% carbonyl iron and 80 wt.% carbonyl iron [278].

SiC-based composites are the most popular selection for high-temperature EMW absorption applications. One prominent example is SiC decorated with NiO-nanorings, which was prepared via chemical deposition of nickel chloride and nickel sulphate on SiC powders and subsequent oxidization of as-prepared powders. The resultant NiO-SiC composites showed a novel hierarchical architecture and exhibit significantly enhanced EMW absorption performance than that of pristine SiC [297]. As can be seen from Figure 20, the minimal RL of NiO-SiC composite reached approximately -50 dB, which was three times better than that of SiC at 673 K, and the EBA covered the entire X band. Furthermore, the EBA of NiO-SiC broadened with increasing temperature. The excellent EMW absorption performance results from multi-relaxation mechanisms: (i) the defect polarization in NiO nanocrystal and SiC grains; (ii) magnetic-dielectric hybrid structure (iii) NiO-SiC hierarchical architecture (iv) multiple interfacial polarization. The remarkable high-temperature EMW absorption is ascribed to the complementary relaxation and conductance of NiO and SiC at different temperatures. In addition to the aforementioned magnetic metal oxides, SiC-based composites decorated by other absorbing materials such as metal particles or conductive carbon, achieve outstanding EMW absorption performance and enhanced EAB at high temperatures [70,298–302].

A graphene@ $\text{Fe}_3\text{O}_4/\text{SiBCN}$ composite is another material suitable for EMW absorbing application under high temperature conditions. This composite was prepared by polymer-derived-ceramic method. It achieved excellent EMW absorption performance in terms of a broad EAB (covering 93.6% range of the X-band at 600°C) and quite low RL at high-temperature conditions, which are much better than those

of previously reported graphene, Fe_3O_4 and SiBCN materials [89]. The outstanding high-temperature EMW absorbing performance is attributed to the synergistic effect due to dielectric loss (free carbon and graphene), and magnetic loss (Fe_3O_4) of the graphene@ $\text{Fe}_3\text{O}_4/\text{SiBCN}$ composites.

Luo et al. investigated the iron-containing SiBCN materials, which showed enhanced EMW absorption performance at 600°C [303]. At this temperature, the minimal RL of a 2.8 mm sample reached -37.87 dB at 10.17 GHz, and the EAB covered the entire X-band. The experimental results clarified that the improved EMW absorption performance has to be attributed to the formation of SiC, Fe_3Si nanocrystals and turbostratic carbon in the SiBCN matrix. At elevated temperatures, more free electrons stemming from SiC, Fe_3Si nanocrystals and turbostratic carbon phase exist, which are advantageous for improving the electrical conductivity and for increasing the imaginary part of the complex permittivity. In addition, there are some boundaries of SiC nanocrystals and graphite carbons in the SiBCN amorphous matrix. These boundaries induce some defects and polarized centres, resulting in the synergistic effect of interfacial polarization and dipole polarization. Moreover, these composites also exhibited good mechanical properties and outstanding high-temperature oxidation resistance up to 885°C in the air.

Furthermore, Xu et al. fabricated a novel red blood cell like-mesoporous carbon hollow microsphere (RBC-PCHMs) composite. The as-obtained RBC-PCHMs composite with a small sample thickness (< 2 mm) showed a broad EAB (> 3 GHz) in the X band at temperatures between RT and 250°C [304]. The investigation on the mechanisms illustrates that the polarization and conduction loss are complementary with rising temperature, which is beneficial for the

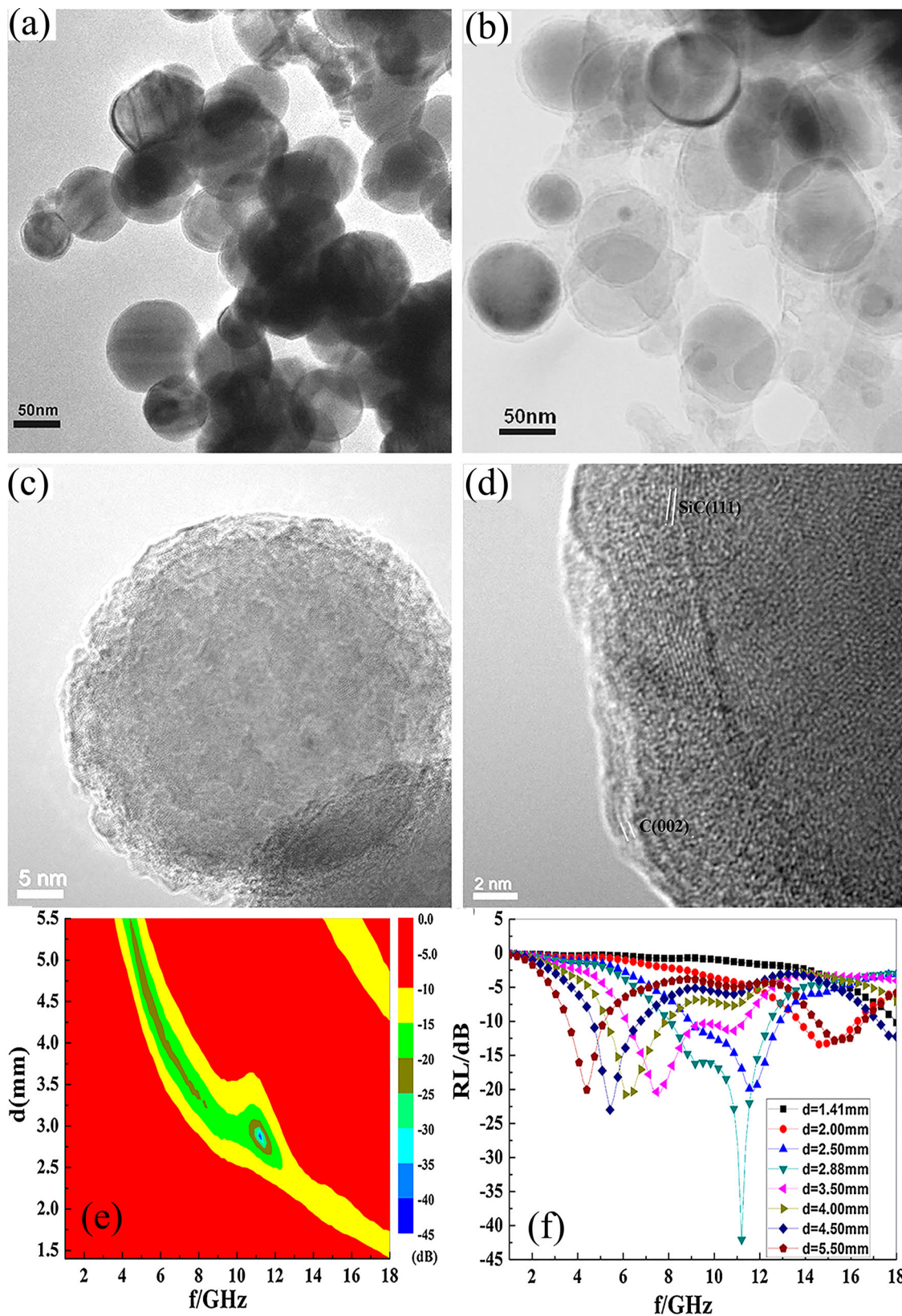


Figure 18. TEM micrographs of Ni nanoparticles (a) and TEM and HRTEM images of Ni@SiC nanocomposites (b-d); (e) two-dimensional RL mapping plots of Ni@SiC; (f) RL of the Ni@SiC composites [280].

creation of high matching impedance and strong EMW attenuation.

Composites comprised of SiO_2 and 2, 5 and 10 wt.% of multiwalled carbon nanotubes (MWCNTs) were fabricated to investigate their dielectric properties

and EMW absorption performance at a broad temperature range from 100 to 500°C. The EAB of the $\text{SiO}_2/\text{MWCNTs}$ composites loaded with 10 wt.% MWCNTs covered the whole X band at the temperature ranging from 100 to 500°C [108]. Table 5

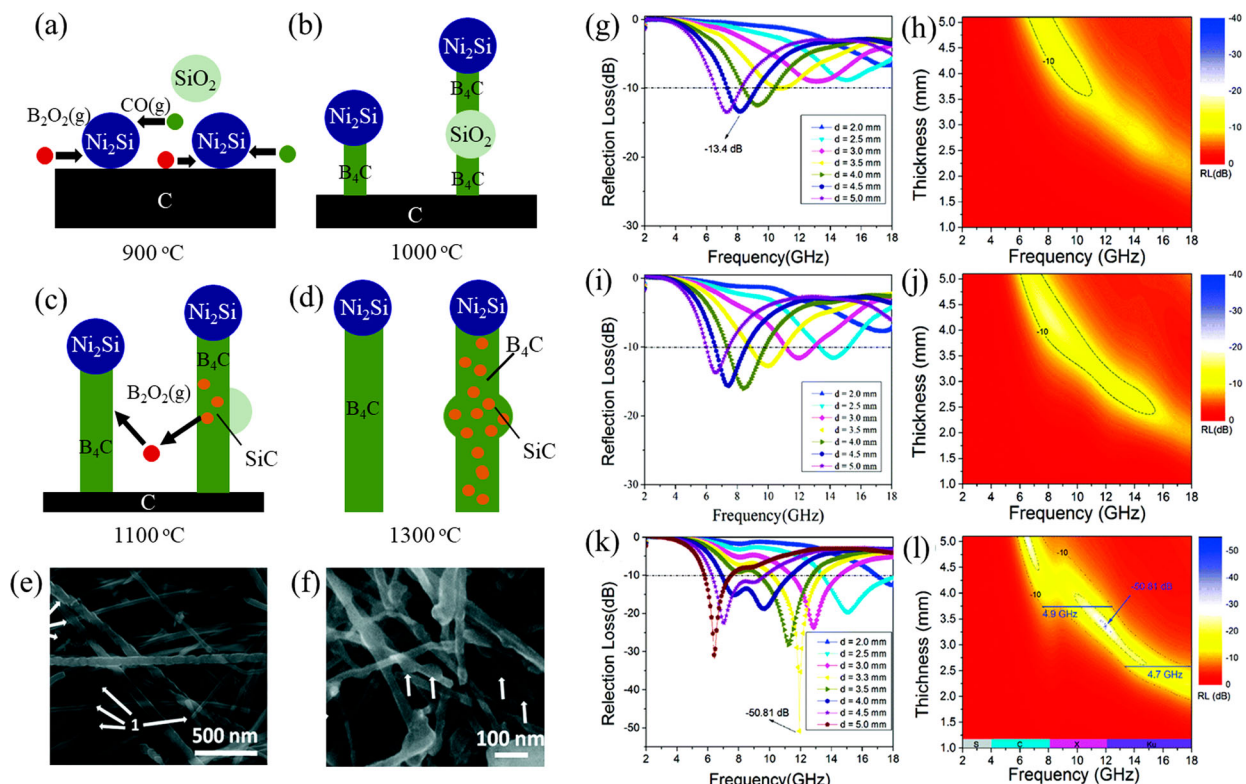


Figure 19. Schematic images of the growth of B₄C and SiC/B₄C nanowires with a C/SiO molar ratio of 1:0.36 (a) 900°C; (b) 1000°C; (c) 1100°C; (d) 1300°C, and SEM images of samples (e) 1100°C and (f) 1300°C; RL curves and the corresponding RL maps of samples with different C/SiO molar ratio (g, h) 1:0.04; (i, j) 1:0.16; (k, l) 1:0.36 [282].

summarizes the EMW absorption performance of ceramic composites at different temperatures.

It is worth noting from Table 5 that ceramics and their composites exhibit excellent EMW absorption performance at temperatures even higher than 300°C. The combination of advanced ceramics and dielectric/magnetic loss phase (e.g. carbonaceous materials, transition metal carbide/nitride/silicide, magnetic metal and their oxides) is a promising strategy for the development of high-temperature resistant EMW absorbing materials.

Lightweight and flexible concepts

In order to meet the requirements of the next-generation flexible electronic devices, EMW absorbing materials should not only have strong absorption capability, but also possess features like flexibility and lightweight. Recently, tremendous progress in EMW absorbing field has been proven that porous materials are regarded as promising flexible, lightweight and high-efficiency absorbers due to their low density, good impedance matching and supported characteristics. Furthermore, high porosity is favourable for enhanced EMW penetrating into the absorbing medium and facilitates multiple reflections inside the absorbing medium. Ceramic foams and aerogels containing suitable fillers are considered as the best combination of EMW absorption capabilities and

mechanical properties because of their efficient optimization of the strength/density ratio.

3D hierarchical lightweight carbon foams modified with Si₃N₄ and SiC were successfully synthesized by carbothermal reduction between carbon foams and nanosilicon and silica under the flowing N₂. [312]. The presence of porosity in materials significantly enhances the EMW absorption performance. The minimal RL reached -43.2 dB at 4.7 GHz with a thickness of 5.0 mm, and the maximum EAB amounted up to 4 GHz (11.8–15.8 GHz) with a thickness of 2.0 mm. The improved EMW absorption capability is proven to be linked with its special structural characteristics such as in situ formed straight nanowires of Si₃N₄, curved nanowires of SiC, pore walls of carbon foams, which all contribute to multiple reflections and polarization relaxation.

Xiao et al. coated nanostructured lamellar carbon films with 3D hybrid foams of SiC nanowires by combining unidirectional freeze drying and carbonization techniques (see Figure 21) [313]. The as-obtained ultralight hybrid foam shows outstanding EMW absorption performance as compared to individual SiC nanowires and carbon. The investigation of the mechanisms illustrates that carbon films and foams are beneficial for the creation of multiple polarization and dielectric loss. Ye et al. prepared an ultrathin 3D reticulated SiC/porous carbon foam composite (3D-SiC/PCF) by combining the carbonization of

Table 4. EMW absorption performance determined by microstructures (ISF: interconnected SiC foam; real part (ϵ') and imaginary part (ϵ'') permittivity are approximate values estimated from the cited literatures).

Materials	Thickness (mm)	Frequency (GHz)	RL (dB)	EAB (GHz)	Complex permittivity		Weight per cent (%)	Matrix	Ref
					Real part (ϵ')	Imaginary part (ϵ'')			
CFs-Si ₃ N ₄ sandwich	5.0	12.4	-14.4	~	7.94–12.21	1.07–5.14	100	~	[284]
SiO ₂ @Fe ₃ O ₄ core/shell nanorod	2.5	~	-32.0	3.0	4.87–7.79	2.84–4.37	20.0	paraffin	[285]
3D-ISF	9.5	9.52	-45.7	2.74	6.21–7.44	0.84–1.89	50	paraffin	[286]
Nano C-SiC	1.66	16.0	-76.6	~	5.39–12.51	3.07–6.37	~	paraffin	[287]
Ni@SiC core–shell spheres	2.0	~	-22.4	8.06	3.07–11.66	0.56–3.11	50	paraffin	[288]
core/shell/shell-like Fe ₃ O ₄ @SiO ₂ @PPy	5.0	6.0	-40.9	6.88	4.02–8.94	1.68–4.14	75	paraffin	[289]
Sandwich-like SiCNW/C/Si ₃ N ₄	2.9	~	-39.7	X band	6.37–7.42	3.04–3.79	100	~	[290]
Fe ₃ Si@C/SiC/Fe ₃ O ₄ /SiO ₂	4.5	4.25	-44.7	~	11.94–17.83	3.81–4.66	50	paraffin	[141]
CNWs-SiO ₂ /3Al ₂ O ₃ -2SiO ₂	5.0	9.1	-31.0	X band	1.91–2.18	1.29–1.57	100	~	[291]
Fe@Carbon dual-shells	4.5	8.8	-54.4	~	8.07–15.71	3.22–4.07	70	paraffin	[292]
bone-like graphene@SiC	3.0	10.52	-47.3	4.7	5.04–10.07	2.11–4.23	50	epoxy	[293]
SiC/SiO ₂ core–shell nanowires	3.0	13.84	-32.7	4.32	3.64–7.08	0.61–3.54	0.5	paraffin	[294]
ErC ₂ @C core–shell structure	2.44	15.00	-49.0	~	4.21–5.74	1.83–1.96	50	paraffin	[295]
SiC/porous carbon foam	1.05	17.20	-25.9	3.24	17.63–22.58	2.52–6.22	~	paraffin	[296]



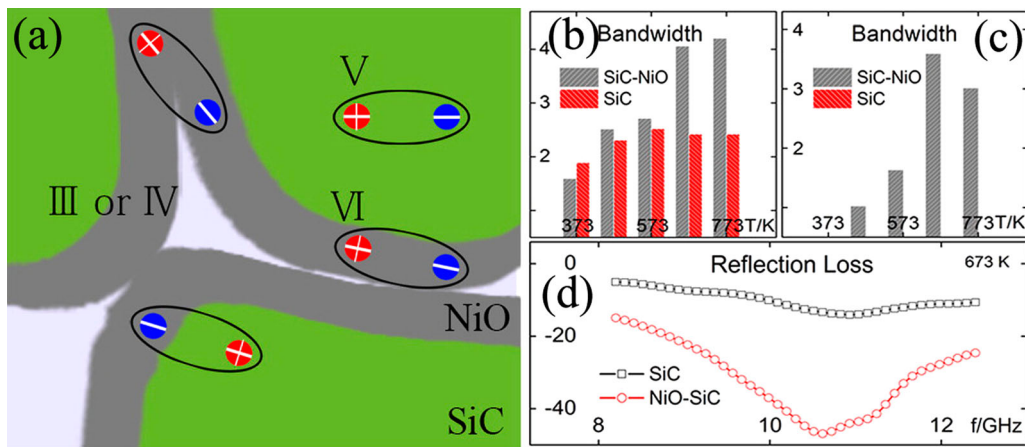


Figure 20. (a) Schematic diagram of dipole polarization in NiO–SiC. Absorption bandwidth of SiC and NiO–SiC at different temperatures at the level of (b) –10 dB and (c) –20 dB, (d) RL of SiC and NiO/SiC (reprinted with permission from American Chemical Society) [297].

melamine foam step with a CVD process. The 3D-SiC/PCF accounts for stronger and larger RL than porous carbon foam in the same frequency range. Other porous ceramic foam composites are summarized in Table 4.

Ceramic aerogels, with ultralight weight, high-temperature oxidation resistance and high specific surface area, have attracted great attention as next-generation EMW absorption materials. Ultralight PDC aerogels (PDCAs) with enhanced EMW absorption properties were fabricated by combining polymer crosslinking via hydrosilylation and subsequent freeze drying of the obtained gel structure [314]. The resultant PDCAs exhibited a homogeneously 3D framework with an extremely low bulk density (0.19 g/cm³) and high specific surface area (134.48 m²/g). Its RL_{min} achieved –42.01 dB at 12.5 GHz with a thickness of 3.0 mm, and a wide EAB (6.6 GHz) is obtained. The excellent EMW absorbing performance is due to

multiple reflections of EMWs in the 3D framework, good impedance matching and high dielectric loss. Shao et al. prepared a Co/SiCN ceramic aerogel composite (Co/SiCN-CACs) with a 3D porous microstructure. It was found that the combination of magnetic Co and 3D porous microstructure not only generates obvious magnetic loss ability and multiple reflections, but also causes typical interfacial polarization [315]. The resultant Co/SiCN-CACs show improved EMW absorption performance as compared with individual Co particles embedded in a SiCN matrix. Zhao et al. fabricated magnetic and conductive Ni/carbon aerogel composites with high surface area, low densities, controllable electrical conductivity and magnetization. The porosity and incorporation of Co were confirmed to be in charge of the improved EMW absorption performance in the frequency range of 2.0–18.0 GHz [316]. However, in general there are presently only few works published related to ceramic aerogels

Table 5. High-temperature EMW absorption performance of ceramic composites (real part (ϵ') and imaginary part (ϵ'') permittivity are approximate values estimated from the cited literatures; stable temperature is the highest temperature for testing).

Materials	Room temperature		High temperature		Complex permittivity		Stable temperature		
	RL (dB)	EAB (GHz)	T/°C	RL (dB)	EAB (GHz)	Real part (ϵ')	Imaginary part (ϵ'')	(°C)	Ref.
graphene@Fe ₃ O ₄ /SiBCN	–43.78	3.2	25–600	–46 at 600°C	2.27–4.13	10.71–12.28	6.68–7.86	1100–1400°C	[89]
nickel chains/SiO ₂	~	9.60	50–300	–50 at 100°C	4.2	6.10–21.20	0.20–5.90	300°C	[305]
Si ₃ N ₄ –SiC/SiO ₂	–38.6	4.03	25–600	–36 at 600°C	4	5.72–6.25	2.81–5.19	600°C	[69]
CF/SiO ₂	–10.2	1.1	30–600	–9 at 600°C	5.24	21.13–29.41	12.51–14.77	600°C	[188]
Al/ZnO/ZrSiO ₄	–15.0	2.9	20–650	–70 at 300°C	3.3	6.30–7.83	3.02–4.71	700°C	[306]
Fe–SiC/SiO ₂	–10.2	~1	25–500	–32 at 500°C	~3.4	5.24–8.07	1.52–3.32	500°C	[301]
Cds-MWCNTs			50–300	–47 at 200°C	2 (<–20 dB)	6.10–12.00	2.40–6.60	300°C	[307]
SiC _f /SiC–Al ₂ O ₃	–15.6	2.7	25–700	–42 at 300°C	3.4	5.50–6.30	1.90–3.10	700°C	[299]
MWCNTs/SiO ₂			100–500	–39 at 500°C	4.2	5.05–7.68	~	500°C	[108]
ZnO–MWCNT/SiO ₂	–20.7	~2.4	50–400	–13 at 400°C	3.4	7.26–10.11	4.82–7.96	400°C	[107]
rGO–SiC/SiOC	–69.3	3.4	20–400	–50 at 400°C	3.9	7.94–9.42	3.26–5.12	400°C	[308]
NiO/SiC			100–500	–50 at 400°C	4.2	11.91–14.82	5.16–7.20	500°C	[309]
CNT-ZnO/glass	–70.0	3.9	20–400	–22 at 400°C	3.2	7.41–8.30	2.60–3.40	400°C	[310]
LAS/LAS-SiC	–48.1	~1.4	300–500	–43 at 300°C	3.9	~	~	500°C	[311]
Iron-containing SiBCN	–21.4	3.26	25–600	–12.6 at 885°C	3.2	6.13–7.39	3.37–3.56	1400°C	[303]
Co–SiC			50–300	–44.7 at 300°C	~3	18.12–23.54	5.19–8.06	300°C	[300]
Mesoporous carbon	–10.7	0.7	27–240	–59.7 at 100°C	3.4	10.21–12.66	5.02–7.98	250°C	[304]
Ni–SiC			100–400	–48 at 400°C	4.2	17.12–21.79	6.17–8.24	250°C	[298]

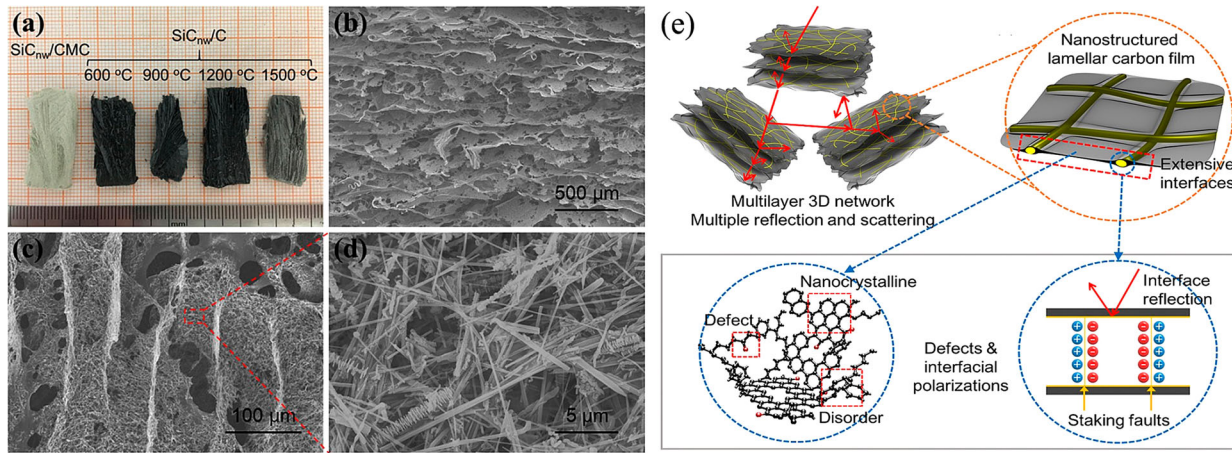


Figure 21. (a) Optical figures of the SiC NWs/CMC foam and the SiC NWs/C foam. SEM images of (b) the SiC NWs/CMC foam top view, (c) SiC NWs/CMC lamella side view, (d) the enlarged SEM image of the SiC NWs/CMC lamella and (e) schematics description of the EMW absorption mechanisms of SiC NWs/C hybrid foams (reprinted with permission of Elsevier) [313].

dealing with EMW absorption features obviously due to challenging synthesis conditions.

Strong and thermostable polymeric graphene/silica textile composites were prepared for light-weight practical EMW absorption applications [186]. The as-fabricated composites containing 4.1 wt.% of reduced graphene oxide (RGO) were lightweight with a low density ($\sim 1 \text{ g/cm}^3$), strong tensile strength of 40 MPa and high thermal stability beyond 225°C in air, coupled with a minimal RL_{\min} of -36 dB and broad EAB in the X band. As shown in Figure 22, this combination strategy allows to obtain excellent efficiency for constituting the advantages of each component into one unit, such as the electrical conductivity of RGO, the thermal stability of the silica textile, and the mechanical strength of the phenol formaldehyde (PF) resin. Most importantly, the complicated interfaces formed by the different components

provide typical interfacial polarization and electric dipole polarization, leading to an excellent EMW absorption compared with those of the single-components.

Conclusion and future perspectives

This review comprehensively introduces recent developments in the field of advanced ceramics and associated composites used as effective EMW absorption materials. According to the different characteristics, EMW absorption materials can be classified into dielectric-loss type and magnetic-loss type materials, corresponding to their characteristic dielectric loss and magnetic loss mechanisms, respectively. Single-component materials (e.g. metals and polymers) are generally not preferred due to their intrinsic disadvantages, especially under high temperature, such as low

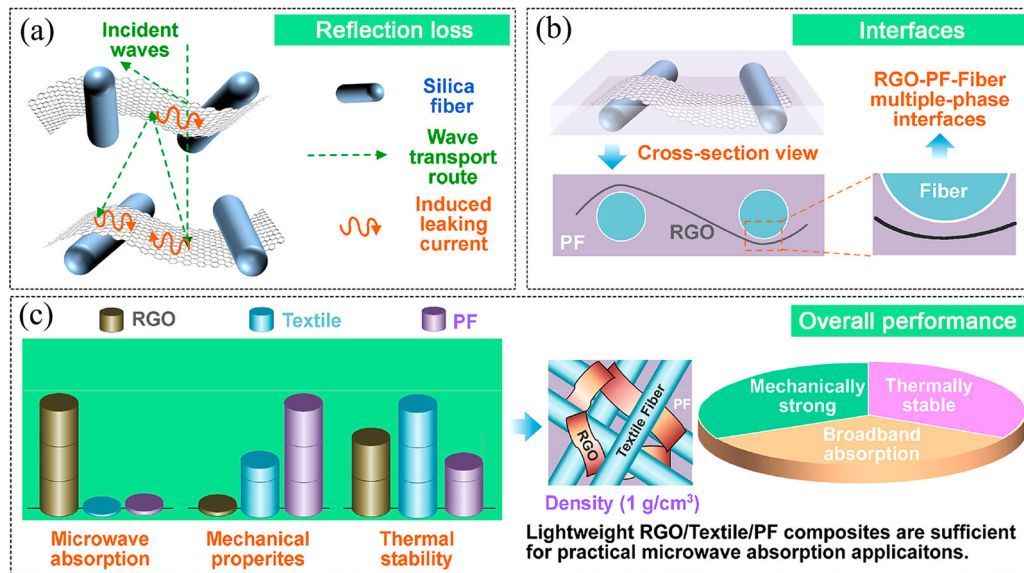


Figure 22. (a) Schematic diagram of RL, (b) the improved mechanism for mechanical strength in the RGO/silica textile/PF composites, and (c) advantageous characteristics from RGO, silica textile and PF (reprinted with permission of Elsevier) [186].

melting point, poor thermal stability, and bad corrosion resistance. Thus, the general trend in materials science is to develop multifunctional composites that utilize the unique properties by the combination of different materials. However, it is not sufficient to improve the EMW absorption performance by adjusting the chemical and phase composition of the composite. Another approach to develop advanced EMW absorbing materials is to consider microstructure and morphology of the constituting phases. The design of the microstructure and morphology of EMW absorption materials makes incident EMWs to generate multiple reflections, scattering and refraction as much as possible to prolong the transmission path. Moreover, particular morphologies (e.g. nano/macro-scale, flower-like, nanoflake, red blood cell-like, etc.) and microstructures (e.g. porous, core–shell, aerogel, foamed, etc.) allow to form high interface area to promote the attenuation of the EMWs via interfacial polarization. In fact, from a point of application view, it is very important to choose a suitable matrix to support the EMW absorption phases. There is no doubt that the single-component ceramics or ceramic composites loading with one or more conductive/magnetic fillers are the most promising candidate materials for EMW absorbing applications.

It is worth mentioning that ceramic-based materials are the most researched materials for EMW absorption applications under relatively high temperature due to their outstanding chemical and thermal stability. Most of the ceramic composites show attractive EMW absorption performances at temperatures above 300°C. Some of them could keep remarkable attenuation with wide bandwidth at temperatures as high as 500°C. More importantly, modifying and doping ceramics can protect other composite constituents (e.g. carbonaceous materials, metal and metal oxides, etc.) from high-temperature atmospheric environments. These are promising strategies for the development of high-temperature EMW absorption materials. Moreover, EMW absorbing materials with flexibility and lightweight become future challenges for the next-generation of flexible electronic devices. Porous ceramics loading suitable magnetic/dielectric fillers have obtained great attention due to the efficient optimization of EMW absorption capabilities, mechanical and thermal properties.

In the past decades, considerable advancements have been made in EMW absorption research of ceramics and composites. However, these materials still face many obvious challenges mainly including the following aspects: (1) Difficulties in establishing a sufficient conducting network in the ceramic matrix; (2) Challenges in tuning the relationship between EMW absorption properties and physical properties; (3) Requirements for design and preparation of flexible and lightweight EMW absorbent materials;

(4) Difficulties in understanding the relationship between temperature and EMW absorption properties; (5) Bottlenecks in processing and practical application of EMW absorbing materials; (6) Problems in solving EMW leakage occurring between the specimen and test holder; (7) Thermal and corrosive stability and lifetime of ceramics and composites should also be worth investigating. Even more challenges still exist about how to understand and tailor the manyfold interrelationship ‘components-morphologies-structures-properties-applications’ in the field of EMW absorption applications.

Disclosure statement

No potential conflict of interest was reported by the author(s).

Funding

Zhaoju Yu thanks the National Natural Science Foundation of China [Nos. 51872246 and 52061135102] and Alexander von Humboldt Foundation for financial support. Wei Li acknowledges the financial support from China Scholarship Council [No. 201907040060] during his stay at TU Darmstadt. Qingbo Wen thanks National Natural Science Foundation of China [No. 52102085], the State Key Laboratory of Powder Metallurgy, Central South University, Changsha, China [No. 621022117] for financial support.

References

- [1] Shahzad F, Alhabeb M, Hatter CB, et al. Electromagnetic interference shielding with 2D transition metal carbides (MXenes). *Science*. **2016**;353(6304):1137–1140.
- [2] Zhang Y, Huang Y, Zhang T, et al. Broadband and tunable high-performance microwave absorption of an ultralight and highly compressible graphene foam. *Adv Mater*. **2015**;27(12):2049–2053.
- [3] Li Q, Zhang Z, Qi L, et al. Toward the application of high frequency electromagnetic wave absorption by carbon nanostructures. *Adv Sci*. **2019**;6(8):1801057–1801080.
- [4] Tian X, Meng F, Meng F, et al. Synergistic enhancement of microwave absorption using hybridized polyaniline@helical CNTs with dual chirality. *ACS Appl Mater Interfaces*. **2017**;9(18):15711–15718.
- [5] Narendra J, Harnadek M. xGnP for electromagnetic interference shielding application. *XG Sci*. **2012**;5:1–11.
- [6] Liu X, Wang L-S, Ma Y, et al. Enhanced microwave absorption properties by tuning cation deficiency of perovskite oxides of two-dimensional LaFeO₃/C composite in X-band. *ACS Appl Mater Interfaces*. **2017**;9(8):7601–7610.
- [7] Liu Q, Cao Q, Bi H, et al. Coni@SiO₂@TiO₂ and CoNi@Air@TiO₂ microspheres with strong wide-band microwave absorption. *Adv Mater*. **2016**;28(3):486–490.
- [8] Dai B, Zhao B, Xie X, et al. Novel two-dimensional Ti₃C₂T_x MXenes/nano-carbon sphere hybrids for

- high-performance microwave absorption. *J Mater Chem C.* **2018**;6(21):5690–5697.
- [9] IEEE. IEEE international electromagnetic compatibility symposium record. 1973 IEEE International Electromagnetic Compatibility Symposium Record, 1973 Jun 20–22; Group, I., Ed. 1973; p. 1–14.
- [10] Johnson PL. Electromagnetic compatibility: compliance with emerging regulations; 1997.
- [11] Assembly P. The potential dangers of electromagnetic fields and their effect on the environment. European Parliament. 2011.
- [12] Sessions PHP. Avoiding potential risks of electromagnetic fields. European Parliament. **2009**.
- [13] Parliament E. Directive 2013/35/EU of the European Parliament and of the Council of 26 June 2013 on the minimum health and safety requirements regarding the exposure of workers to the risks arising from physical agents (electromagnetic fields). Official J Eur Union. **2009**;179:1–21.
- [14] Sankaran S, Deshmukh K, Ahamed MB, et al. Recent advances in electromagnetic interference shielding properties of metal and carbon filler reinforced flexible polymer composites: a review. *Compos Part A Appl Sci Manuf.* **2018**;114:49–71.
- [15] Meng F, Wang H, Huang F, et al. Graphene-based microwave absorbing composites: a review and prospective. *Compos Part B Eng.* **2018**;137:260–277.
- [16] Lv H, Yang Z, Xu H, et al. An electrical switch-driven flexible electromagnetic absorber. *Adv Funct Mater.* **2020**;30(4):1907251–1907259.
- [17] Lee DW, Park J, Kim BJ, et al. Enhancement of electromagnetic interference shielding effectiveness with alignment of spinnable multiwalled carbon nanotubes. *Carbon.* **2019**;142:528–534.
- [18] Cao M-S, Cai Y-Z, He P, et al. 2D MXenes: electromagnetic property for microwave absorption and electromagnetic interference shielding. *Chem Eng J.* **2019**;359:1265–1302.
- [19] Cheng H, Wei S, Ji Y, et al. Synergetic effect of Fe_3O_4 nanoparticles and carbon on flexible poly (vinylidene fluoride) based films with higher heat dissipation to improve electromagnetic shielding. *Compos Part A Appl Sci Manuf.* **2019**;121:139–148.
- [20] Li N, Xie X, Lu H, et al. Novel two-dimensional $\text{Ti}_3\text{C}_2\text{T}_x/\text{Ni}$ -spheres hybrids with enhanced microwave absorption properties. *Ceram Int.* **2019**;45(17, Part B):22880–22888.
- [21] Shen Z, Chen J, Li B, et al. Recent progress in SiC nanowires as electromagnetic microwaves absorbing materials. *J Alloys Compd.* **2020**;815:152388–152402.
- [22] Wang Y, Du Y, Xu P, et al. Recent advances in conjugated polymer-based microwave absorbing materials. *Polymers.* **2017**;9(1):1–28.
- [23] Zhao H, Cheng Y, Liu W, et al. Biomass-derived porous carbon-based nanostructures for microwave absorption. *Nano-Micro Lett.* **2019**;11(1):1–17.
- [24] Bhattacharjee Y, Arief I, Bose S. Recent trends in multi-layered architectures towards screening electromagnetic radiation: challenges and perspectives. *J Mater Chem C.* **2017**;5(30):7390–7403.
- [25] Bai T, Guo Y, Liu H, et al. Achieving enhanced electromagnetic shielding and absorption capacity of cellulose-derived carbon aerogels via tuning the carbonization temperature. *J Mater Chem C.* **2020**;8(15):5191–5201.
- [26] Yang M, Yuan Y, Li Y, et al. Dramatically enhanced electromagnetic wave absorption of hierarchical CNT/Co/C fiber derived from cotton and metal-organic-framework. *Carbon.* **2020**;161:517–527.
- [27] Elhassan A, Abdalla I, Yu J, et al. Microwave-assisted fabrication of sea cucumber-like hollow structured composite for high-performance electromagnetic wave absorption. *Chem Eng J.* **2020**;392:123646–123656.
- [28] Li C, Sui J, Jiang X, et al. Efficient broadband electromagnetic wave absorption of flower-like nickel/carbon composites in 2–40 GHz. *Chem Eng J.* **2020**;385:123882–123893.
- [29] Liu D, Du Y, Wang F, et al. MOFs-derived multi-chamber carbon microspheres with enhanced microwave absorption. *Carbon.* **2020**;157:478–485.
- [30] Wu G, Zhang H, Luo X, et al. Investigation and optimization of $\text{Fe}/\text{ZnFe}_2\text{O}_4$ as a wide-band electromagnetic absorber. *J Colloid Interface Sci.* **2019**;536:548–555.
- [31] Hou T, Wang B, Jia Z, et al. A review of metal oxide-related microwave absorbing materials from the dimension and morphology perspective. *J Mater Sci Mater Electron.* **2019**;30(12):10961–10984.
- [32] Jiang D, Murugadoss V, Wang Y, et al. Electromagnetic interference shielding polymers and nanocomposites – a review. *Polym Rev.* **2019**;59(2):280–337.
- [33] Kong LB, Li ZW, Liu L, et al. Recent progress in some composite materials and structures for specific electromagnetic applications. *Int Mater Rev.* **2013**;58(4):203–259.
- [34] Jia Z, Lan D, Lin K, et al. Progress in low-frequency microwave absorbing materials. *J Mater Sci Mater Electron.* **2018**;29(20):17122–17136.
- [35] Qin F, Brosseau C. A review and analysis of microwave absorption in polymer composites filled with carbonaceous particles. *J Appl Phys.* **2012**;111(6):061301–061325.
- [36] Quan B, Liang X, Ji G, et al. Dielectric polarization in electromagnetic wave absorption: review and perspective. *J Alloys Compd.* **2017**;728:1065–1075.
- [37] Wang C, Murugadoss V, Kong J, et al. Overview of carbon nanostructures and nanocomposites for electromagnetic wave shielding. *Carbon.* **2018**;140:696–733.
- [38] Yin X, Kong L, Zhang L, et al. Electromagnetic properties of Si-C-N based ceramics and composites. *Int Mater Rev.* **2014**;59(6):326–355.
- [39] Yang H, Ye T, Lin Y, et al. Microwave absorbing properties of the ferrite composites based on graphene. *J Alloys Compd.* **2016**;683:567–574.
- [40] Chandra Babu Naidu K, Madhuri W. Microwave processed bulk and nano NiMg ferrites: a comparative study on X-band electromagnetic interference shielding properties. *Mater Chem Phys.* **2017**;187:164–176.
- [41] Li L, Chen K, Liu H, et al. Attractive microwave-absorbing properties of $\text{M}-\text{BaFe}_{12}\text{O}_{19}$ ferrite. *J Alloys Compd.* **2013**;557:11–17.
- [42] Zhu W, Wang L, Zhao R, et al. Electromagnetic and microwave-absorbing properties of magnetic nickel ferrite nanocrystals. *Nanoscale.* **2011**;3(7):2862–2864.
- [43] Xie J, Han M, Chen L, et al. Microwave-absorbing properties of NiCoZn spinel ferrites. *J Magn Magn Mater.* **2007**;314(1):37–42.
- [44] Xiong J, Xiang Z, Zhao J, et al. Layered NiCo alloy nanoparticles/nanoporous carbon composites

- derived from bimetallic MOFs with enhanced electromagnetic wave absorption performance. *Carbon*. **2019**;154:391–401.
- [45] Liu X, Hao C, Jiang H, et al. Hierarchical $\text{NiCo}_2\text{O}_4/\text{Co}_3\text{O}_4/\text{NiO}$ porous composite: a lightweight electromagnetic wave absorber with tunable absorbing performance. *J Mater Chem C*. **2017**;5(15):3770–3778.
- [46] Wu H, Qin M, Zhang L. NiCo_2O_4 constructed by different dimensions of building blocks with superior electromagnetic wave absorption performance. *Compos Part B Eng*. **2020**;182:107620–107630.
- [47] Qin M, Liang H, Zhao X, et al. Filter paper templated one-dimensional $\text{NiO}/\text{NiCo}_2\text{O}_4$ microrod with wide-band electromagnetic wave absorption capacity. *J Colloid Interface Sci*. **2020**;566:347–356.
- [48] Yang CC, Gung YJ, Hung WC, et al. Infrared and microwave absorbing properties of $\text{BaTiO}_3/\text{polyaniline}$ and $\text{BaFe}_{12}\text{O}_{19}/\text{polyaniline}$ composites. *Compos Sci Technol*. **2010**;70(3):466–471.
- [49] Hosseini SH, Mohseni SH, Asadnia A, et al. Synthesis and microwave absorbing properties of polyaniline/ MnFe_2O_4 nanocomposite. *J Alloys Compd*. **2011**;509(14):4682–4687.
- [50] Wei J, Liu J, Li S. Electromagnetic and microwave absorption properties of Fe_3O_4 magnetic films plated on hollow glass spheres. *J Magn Magn Mater*. **2007**;312(2):414–417.
- [51] Wang L, Guan Y, Qiu X, et al. Efficient ferrite/Co/porous carbon microwave absorbing material based on ferrite@metal-organic framework. *Chem Eng J*. **2017**;326:945–955.
- [52] Feng Y, Qiu T. Preparation, characterization and microwave absorbing properties of FeNi alloy prepared by gas atomization method. *J Alloys Compd*. **2012**;513:455–459.
- [53] Li X, Han X, Tan Y, et al. Preparation and microwave absorption properties of Ni-B alloy-coated Fe_3O_4 particles. *J Alloys Compd*. **2008**;464(1):352–356.
- [54] Bibi M, Abbas SM, Ahmad N, et al. Microwaves absorbing characteristics of metal ferrite/multiwall carbon nanotubes nanocomposites in X-band. *Compos Part B Eng*. **2017**;114:139–148.
- [55] Wang J, Wang J, Xu R, et al. Enhanced microwave absorption properties of epoxy composites reinforced with $\text{Fe}_{50}\text{Ni}_{50}$ -functionalized graphene. *J Alloys Compd*. **2015**;653:14–21.
- [56] Lakshmi K, John H, Mathew KT, et al. Microwave absorption, reflection and EMI shielding of PU-PANI composite. *Acta Mater*. **2009**;57(2):371–375.
- [57] Munir A. Microwave radar absorbing properties of multiwalled carbon nanotubes polymer composites: a review. *Adv Polym Technol*. **2017**;36(3):362–370.
- [58] Ohlan A, Singh K, Chandra A, et al. Microwave absorption behavior of core-shell structured poly(3,4-ethylenedioxy thiophene)-barium ferrite nanocomposites. *ACS Appl Mater Interfaces*. **2010**;2(3):927–933.
- [59] Zhang X-J, Wang G-S, Cao W-Q, et al. Enhanced microwave absorption property of reduced graphene oxide (RGO)- MnFe_2O_4 nanocomposites and polyvinylidene fluoride. *ACS Appl Mater Interfaces*. **2014**;6(10):7471–7478.
- [60] Chiu S-C, Yu H-C, Li Y-Y. High electromagnetic wave absorption performance of silicon carbide nanowires in the gigahertz range. *J Phys Chem C*. **2010**;114(4):1947–1952.
- [61] Kassiba A, Tabellout M, Charpentier S, et al. Conduction and dielectric behaviour of SiC nano-sized materials. *Solid State Commun*. **2000**;115(7):389–393.
- [62] Li X, Zhang L, Yin X, et al. Effect of chemical vapor infiltration of SiC on the mechanical and electromagnetic properties of Si_3N_4 -SiC ceramic. *Scr Mater*. **2010**;63(6):657–660.
- [63] Zhang B, Li J, Sun J, et al. Nanometer silicon carbide powder synthesis and its dielectric behavior in the GHz range. *J Eur Ceram Soc*. **2002**;22(1):93–99.
- [64] Yang H, Cao M, Li Y, et al. Enhanced dielectric properties and excellent microwave absorption of SiC powders driven with NiO nanorings. *Adv Opt Mater*. **2014**;2(3):214–219.
- [65] Jian X, Tian W, Li J, et al. High-Temperature oxidation-resistant $\text{ZrN}_{0.4}\text{B}_{0.6}/\text{SiC}$ nanohybrid for enhanced microwave absorption. *ACS Appl Mater Interfaces*. **2019**;11(17):15869–15880.
- [66] Hou Y, Cheng L, Zhang Y, et al. Enhanced flexibility and microwave absorption properties of HfC/SiC nanofiber mats. *ACS Appl Mater Interfaces*. **2018**;10(35):29876–29883.
- [67] Hou Y, Cheng L, Zhang Y, et al. Electrospinning of Fe/SiC hybrid fibers for highly efficient microwave absorption. *ACS Appl Mater Interfaces*. **2017**;9(8):7265–7271.
- [68] Wei S, Guan L, Song B, et al. Seeds-induced synthesis of SiC by microwave heating. *Ceram Int*. **2019**;45(8):9771–9775.
- [69] Li M, Yin X, Zheng G, et al. High-temperature dielectric and microwave absorption properties of Si_3N_4 -SiC/SiO₂ composite ceramics. *J Mater Sci*. **2015**;50(3):1478–1487.
- [70] Zhou W, Yin R-m, Long L, et al. Enhanced high-temperature dielectric properties and microwave absorption of SiC nanofibers modified Si_3N_4 ceramics within the gigahertz range. *Ceram Int*. **2018**;44(11):12301–12307.
- [71] Ye F, Song Q, Zhang Z, et al. Direct growth of edge-rich graphene with tunable dielectric properties in porous Si_3N_4 ceramic for broadband high-performance microwave absorption. *Adv Funct Mater*. **2018**;28(17):1707205–1707215.
- [72] Zheng G, Yin X, Wang J, et al. Complex permittivity and microwave absorbing property of Si_3N_4 -SiC composite ceramic. *J Mater Sci Technol*. **2012**;28(8):745–750.
- [73] Luo H, Chen W, Zhou W, et al. Carbon fiber/ Si_3N_4 composites with SiC nanofiber interphase for enhanced microwave absorption properties. *Ceram Int*. **2017**;43(15):12328–12332.
- [74] Zhu J, Wei S, Zhang L, et al. Electrical and dielectric properties of polyaniline-Al₂O₃ nanocomposites derived from various Al₂O₃ nanostructures. *J Mater Chem*. **2011**;21(11):3952–3959.
- [75] Wang Y, Luo F, Wei P, et al. Enhanced dielectric properties and high-temperature microwave absorption performance of Zn-doped Al₂O₃ ceramic. *J Electron Mater*. **2015**;44(7):2353–2358.
- [76] Mei H, Zhao X, Zhou S, et al. 3D-printed oblique honeycomb Al₂O₃/SiCw structure for electromagnetic wave absorption. *Chem Eng J*. **2019**;372:940–945.
- [77] Zhou L, Su G, Wang H, et al. Influence of NiCrAlY content on dielectric and microwave absorption

- properties of NiCrAlY/Al₂O₃ composite coatings. *J Alloys Compd.* **2019**;777:478–484.
- [78] Wang Y, Lai Y, Wang S, et al. Controlled synthesis and electromagnetic wave absorption properties of core-shell Fe₃O₄@SiO₂ nanospheres decorated graphene. *Ceram Int.* **2017**;43(2):1887–1894.
- [79] Liu X, Chen Y, Hao C, et al. Graphene-enhanced microwave absorption properties of Fe₃O₄/SiO₂ nanorods. *Compos Part A App Sci Manuf.* **2016**;89:40–46.
- [80] Chen M, Zhu Y, Pan Y, et al. Gradient multilayer structural design of CNTs/SiO₂ composites for improving microwave absorbing properties. *Mater Des.* **2011**;32(5):3013–3016.
- [81] Li S, Huang Y, Zhang N, et al. Synthesis of polypyrrrole decorated FeCo@SiO₂ as a high-performance electromagnetic absorption material. *J Alloys Compd.* **2019**;774:532–539.
- [82] Duan W, Yin X, Ye F, et al. Synthesis and EMW absorbing properties of nano SiC modified PDC-SiOC. *J Mater Chem C.* **2016**;4(25):5962–5969.
- [83] Du B, He C, Shui A, et al. Microwave-absorption properties of heterostructural SiC nanowires/SiOC ceramic derived from polysiloxane. *Ceram Int.* **2019**;45(1):1208–1214.
- [84] Duan W, Yin X, Li Q, et al. Synthesis and microwave absorption properties of SiC nanowires reinforced SiOC ceramic. *J Eur Ceram Soc.* **2014**;34(2):257–266.
- [85] Duan W, Yin X, Luo C, et al. Microwave-absorption properties of SiOC ceramics derived from novel hyperbranched ferrocene-containing polysiloxane. *J Eur Ceram Soc.* **2017**;37(5):2021–2030.
- [86] Qin H, Liu Y, Ye F, et al. Dielectric and microwave absorption properties of SiCnw-SiBCN composite ceramics deposited via chemical vapor infiltration. *J Alloys Compd.* **2019**;771:747–754.
- [87] Ye F, Zhang L, Yin X, et al. Dielectric and EMW absorbing properties of PDCs-SiBCN annealed at different temperatures. *J Eur Ceram Soc.* **2013**;33(8):1469–1477.
- [88] Ye F, Zhang L, Yin X, et al. Dielectric and microwave-absorption properties of SiC nanoparticle/SiBCN composite ceramics. *J Eur Ceram Soc.* **2014**;34(2):205–215.
- [89] Luo C, Jiao T, Gu J, et al. Graphene shield by SiBCN ceramic: a promising high-temperature electromagnetic wave-absorbing material with oxidation resistance. *ACS Appl Mater Interfaces.* **2018**;10(45):39307–39318.
- [90] Zhu Y-F, Zhang L, Natsuki T, et al. Facile synthesis of BaTiO₃ nanotubes and their microwave absorption properties. *ACS Appl Mater Interfaces.* **2012**;4(4):2101–2106.
- [91] Yang J, Zhang J, Liang C, et al. Ultrathin BaTiO₃ nanowires with high aspect ratio: a simple one-step hydrothermal synthesis and their strong microwave absorption. *ACS Appl Mater Interfaces.* **2013**;5(15):7146–7151.
- [92] Huang X, Chen Z, Tong L, et al. Preparation and microwave absorption properties of BaTiO₃@MWCNTs core/shell heterostructure. *Mater Lett.* **2013**;111:24–27.
- [93] Shi G-M, Li Y-F, Ai L, et al. Two step synthesis and enhanced microwave absorption properties of polycrystalline BaTiO₃ coated Ni nanocomposites. *J Alloys Compd.* **2016**;680:735–743.
- [94] Liu Y, Luo F, Zhou W, et al. Dielectric and microwave absorption properties of Ti₃SiC₂ powders. *J Alloys Compd.* **2013**;576:43–47.
- [95] Liu Y, Su X, Luo F, et al. Facile synthesis and microwave absorption properties of double loss Ti₃SiC₂/Co₃Fe₇ powders. *Ceram Int.* **2018**;44(2):1995–2001.
- [96] Liu Y, Luo F, Wang Y, et al. Influences of milling on the dielectric and microwave absorption properties of Ti₃SiC₂/cordierite composite ceramics. *J Alloys Compd.* **2015**;629:208–213.
- [97] Liu Y, Luo F, Su J, et al. Dielectric and microwave absorption properties of Ti₃SiC₂/cordierite composite ceramics oxidized at high temperature. *J Alloys Compd.* **2015**;632:623–628.
- [98] Rao CNR, Gopalakrishnan K. Borocarbonitrides, BxCyNz: synthesis, characterization, and properties with potential applications. *ACS Appl Mater Interfaces.* **2017**;9(23):19478–19494.
- [99] Zhang T, Zeng S, Wen G, et al. Novel carbon nanofibers build boron carbonitride porous architectures with microwave absorption properties. *Microporous Mesoporous Mater.* **2015**;211:142–146.
- [100] Zhang T, Zhang J, Luo H, et al. Facile approach to fabricate BCN/Fe_x(B/C/N)_y nano-architectures with enhanced electromagnetic wave absorption. *Nanotechnology.* **2018**;29(23):235701–235712.
- [101] Zhao Z, Jia Z, Wu H, et al. Morphology-dependent electromagnetic wave absorbing properties of iron-based absorbers: one-dimensional, two-dimensional, and three-dimensional classification. *The Euro Phys J Appl Phys.* **2019**;87(2):20901–20920.
- [102] Jia Y, Chowdhury MAR, Zhang D, et al. Wide-band tunable microwave-absorbing ceramic composites made of polymer-derived SiOC ceramic and in situ partially surface-oxidized ultra-high-temperature ceramics. *ACS Appl Mater Interfaces.* **2019**;11(49):45862–45874.
- [103] Liu Z, Bai G, Huang Y, et al. Microwave absorption of single-walled carbon nanotubes/soluble cross-linked polyurethane composites. *J Phys Chem C.* **2007**;111(37):13696–13700.
- [104] Ma Z, Zhang Y, Cao C, et al. Attractive microwave absorption and the impedance match effect in zinc oxide and carbonyl iron composite. *Phys B.* **2011**;406(24):4620–4624.
- [105] Abdi MM, Kassim AB, Ekramul Mahmud HNM, et al. Electromagnetic interference shielding effectiveness of new conducting polymer composite. *J Macromol Sci, Part A.* **2009**;47(1):71–75.
- [106] Ren F, Yu H, Wang L, et al. Current progress on the modification of carbon nanotubes and their application in electromagnetic wave absorption. *RSC Adv.* **2014**;4(28):14419–14431.
- [107] Lu M-M, Cao W-Q, Shi H-L, et al. Multi-wall carbon nanotubes decorated with ZnO nanocrystals: mild solution-process synthesis and highly efficient microwave absorption properties at elevated temperature. *J Mater Chem A.* **2014**;2(27):10540–10547.
- [108] Wen B, Cao M-S, Hou Z-L, et al. Temperature dependent microwave attenuation behavior for carbon-nanotube/silica composites. *Carbon.* **2013**;65:124–139.
- [109] Dakin TW. Conduction and polarization mechanisms and trends in dielectric. *IEEE Electr Insul Mag.* **2006**;22(5):11–28.

- [110] Ding D, Wang Y, Li X, et al. Rational design of core-shell Co@C microspheres for high-performance microwave absorption. *Carbon*. **2017**;111:722–732.
- [111] Ohlan A, Singh K, Chandra A, et al. Microwave absorption behavior of core–shell structured poly(3,4-ethylenedioxy thiophene)–barium ferrite nanocomposites. *ACS Appl Mater Interfaces*. **2010**;2(3):927–933.
- [112] Zhu J, Gu H, Luo Z, et al. Carbon nanostructure-derived polyaniline metacomposites: electrical, dielectric, and giant magnetoresistive properties. *Langmuir*. **2012**;28(27):10246–10255.
- [113] Phang S-W, Hino T, Abdullah MH, et al. Applications of polyaniline doubly doped with p-toluene sulphonic acid and dichloroacetic acid as microwave absorbing and shielding materials. *Mater Chem Phys*. **2007**;104(2):327–335.
- [114] Sun K, Xie P, Wang Z, et al. Flexible polydimethylsiloxane/multi-walled carbon nanotubes membranous metacomposites with negative permittivity. *Polymer*. **2017**;125:50–57.
- [115] Zhou Y, Wang N, Qu X, et al. Arc-discharge synthesis of nitrogen-doped C embedded TiCN nanocubes with tunable dielectric/magnetic properties for electromagnetic absorbing applications. *Nanoscale*. **2019**;11(42):19994–20005.
- [116] Koops CG. On the dispersion of resistivity and dielectric constant of some semiconductors at audio-frequencies. *Phys Rev*. **1951**;83(1):121–124.
- [117] González M, Pozuelo J, Baselga J. Electromagnetic shielding materials in GHz range. *Chem Rec*. **2018**;18(7–8):1000–1009.
- [118] Meng F, Wei W, Chen X, et al. Design of porous C@Fe₃O₄ hybrid nanotubes with excellent microwave absorption. *Phys Chem Chem Phys*. **2016**;18(4):2510–2516.
- [119] Wu M, Zhang YD, Hui S, et al. Microwave magnetic properties of Co₅₀/(SiO₂)₅₀ nanoparticles. *Appl Phys Lett*. **2002**;80(23):4404–4406.
- [120] Wu T, Liu Y, Zeng X, et al. Facile hydrothermal synthesis of Fe₃O₄/C core-shell nanorings for efficient low-frequency microwave absorption. *ACS Appl Mater Interfaces*. **2016**;8(11):7370–7380.
- [121] Lu B, Dong XL, Huang H, et al. Microwave absorption properties of the core/shell-type iron and nickel nanoparticles. *J Magn Magn Mater*. **2008**;320(6):1106–1111.
- [122] Zhao Y, Liu L, Jiang K, et al. Distinctly enhanced permeability and excellent microwave absorption of expanded graphite/Fe₃O₄ nanoring composites. *RSC Adv*. **2017**;7(19):11561–11567.
- [123] Kim S-S, Kim S-T, Yoon Y-C, et al. Magnetic, dielectric, and microwave absorbing properties of iron particles dispersed in rubber matrix in gigahertz frequencies. *J Appl Phys*. **2005**;97(10):10F905–10F908.
- [124] Gao B, Qiao L, Wang J, et al. Microwave absorption properties of the Ni nanowires composite. *J Phys D Appl Phys*. **2008**;41(23):235005–235010.
- [125] Micheli D, Pastore R, Vricella A, et al. Electromagnetic characterization of materials by vector network analyzer experimental setup. In: Zachariah AK, Mishra RK, Thomas R, editors. *Spectroscopic methods for nanomaterials characterization*. Amsterdam: Elsevier; **2017**. p. 195–236.
- [126] Michielssen E, Sajer J, Ranjithan S, et al. Design of lightweight, broad-band microwave absorbers using genetic algorithms. *IEEE Trans Microwave Theory Tech*. **1993**;41(6):1024–1031.
- [127] Lv H, Ji G, Liang X, et al. A novel rod-like MnO₂@Fe loading on graphene giving excellent electromagnetic absorption properties. *J Mater Chem C*. **2015**;3(19):5056–5064.
- [128] Du Y, Liu W, Qiang R, et al. Shell thickness-dependent microwave absorption of core-shell Fe₃O₄@C composites. *ACS Appl Mater Interfaces*. **2014**;6(15):12997–13006.
- [129] Cheng Y, Zhao Y, Zhao H, et al. Engineering morphology configurations of hierarchical flower-like MoSe₂ spheres enable excellent low-frequency and selective microwave response properties. *Chem Eng J*. **2019**;372:390–398.
- [130] Li Q, Yin X, Duan W, et al. Electrical, dielectric and microwave-absorption properties of polymer derived SiC ceramics in X band. *J Alloys Compd*. **2013**;565:66–72.
- [131] Dong S, Zhang X, Zhang D, et al. Strong effect of atmosphere on the microstructure and microwave absorption properties of porous SiC ceramics. *J Eur Ceram Soc*. **2018**;38(1):29–39.
- [132] Guo X, Feng Y, Lin X, et al. The dielectric and microwave absorption properties of polymer-derived SiCN ceramics. *J Eur Ceram Soc*. **2018**;38(4):1327–1333.
- [133] Wen Q, Yu Z, Riedel R. The fate and role of in situ formed carbon in polymer-derived ceramics. *Prog Mater Sci*. **2020**;109:100623–100686.
- [134] Liu Q, Zi Z, Zheng Q, et al. Large-scale synthesis, characterization, and microwave absorption properties of manganese oxide nanowires. *Integr Ferroelectr*. **2015**;164(1):82–89.
- [135] Yan D, Cheng S, Zhuo RF, et al. Nanoparticles and 3D sponge-like porous networks of manganese oxides and their microwave absorption properties. *Nanotechnology*. **2009**;20(10):105706–105716.
- [136] Guan H, Chen G, Zhang S, et al. Microwave absorption characteristics of manganese dioxide with different crystalline phase and nanostructures. *Mater Chem Phys*. **2010**;124(1):639–645.
- [137] Wu F, Xia Y, Wang Y, et al. Two-step reduction of self-assembled three-dimensional (3D) reduced graphene oxide (RGO)/zinc oxide (ZnO) nanocomposites for electromagnetic absorption. *J Mater Chem A*. **2014**;2(47):20307–20315.
- [138] Yuchang Q, Qinlong W, Fa L, et al. Temperature dependence of the electromagnetic properties of graphene nanosheet reinforced alumina ceramics in the X-band. *J Mater Chem C*. **2016**;4(22):4853–4862.
- [139] Qing Y, Nan H, Luo F, et al. Nitrogen-doped graphene and titanium carbide nanosheet synergistically reinforced epoxy composites as high-performance microwave absorbers. *RSC Adv*. **2017**;7(44):27755–27761.
- [140] Song C, Cheng L, Liu Y, et al. Microstructure and electromagnetic wave absorption properties of RGO-SiBCN composites via PDC technology. *Ceram Int*. **2018**;44(15):18759–18769.
- [141] Gu C, Guo C, Dong X, et al. Core-shell structured iron-containing ceramic nanoparticles: facile fabrication and excellent electromagnetic absorption properties. *J Am Ceram Soc*. **2019**;102(12):7098–7107.
- [142] Wen Q, Feng Y, Yu Z, et al. Microwave absorption of SiC/HfC_xN_{1-x}/C ceramic nanocomposites with HfC_xN_(1-x)-carbon core-shell particles. *J Am Ceram Soc*. **2016**;99(8):2655–2663.



- [143] Feng Y, Yang Y, Wen Q, et al. Dielectric properties and electromagnetic wave absorbing performance of single-source-precursor synthesized $\text{Mo}_{4.8}\text{Si}_3\text{C}_{0.6}/\text{SiC/C}_{\text{free}}$ nanocomposites with an in situ formed Nowotny phase. *ACS Appl Mater Interfaces*. **2020**;12(14):16912–16921.
- [144] Dai S, Cheng Y, Quan B, et al. Porous-carbon-based Mo_2C nanocomposites as excellent microwave absorber: a new exploration. *Nanoscale*. **2018**;10(15):6945–6953.
- [145] Shrestha G, Traina S, Swanston C. Black carbon's properties and role in the environment: a comprehensive review. *Sustainability*. **2010**;2(1):294–320.
- [146] Fan Y, Yang H, Li M, et al. Evaluation of the microwave absorption property of flake graphite. *Mater Chem Phys*. **2009**;115(2):696–698.
- [147] Li G, Xie T, Yang S, et al. Microwave absorption enhancement of porous carbon fibers compared with carbon nanofibers. *J Phys Chem C*. **2012**;116(16):9196–9201.
- [148] Wan F, Luo F, Wang H, et al. Effects of carbon black (CB) and alumina oxide on the electromagnetic- and microwave-absorption properties of SiC fiber/aluminum phosphate matrix composites. *Ceram Int*. **2014**;40(10):15849–15857.
- [149] Zhang Z, Chen X, Wang Z, et al. Carbonyl iron/graphite microspheres with good impedance matching for ultra-broadband and highly efficient electromagnetic absorption. *Opt Mater Express*. **2018**;8(11):3319–3331.
- [150] Zhong B, Liu W, Yu Y, et al. Enhanced microwave absorption properties of graphite nanoflakes by coating hexagonal boron nitride nanocrystals. *Appl Surf Sci*. **2017**;420:858–867.
- [151] Xie W, Zhu X, Yi S, et al. Electromagnetic absorption properties of natural microcrystalline graphite. *Mater Des*. **2016**;90:38–46.
- [152] Joseph N, Varghese J, Sebastian MT. Graphite reinforced polyvinylidene fluoride composites an efficient and sustainable solution for electromagnetic pollution. *Compos Part B Eng*. **2017**;123:271–278.
- [153] Wang P, Cheng L, Zhang Y, et al. Electrospinning of graphite/SiC hybrid nanowires with tunable dielectric and microwave absorption characteristics. *Compos Part A Appl Sci Manuf*. **2018**;104:68–80.
- [154] Wang P, Cheng L, Zhang L. One-dimensional carbon/SiC nanocomposites with tunable dielectric and broadband electromagnetic wave absorption properties. *Carbon*. **2017**;125:207–220.
- [155] Xiang J, Li J, Zhang X, et al. Magnetic carbon nanofibers containing uniformly dispersed Fe/Co/Ni nanoparticles as stable and high-performance electromagnetic wave absorbers. *J Mater Chem A*. **2014**;2(40):16905–16914.
- [156] Park K-Y, Han J-H, Lee S-B, et al. Microwave absorbing hybrid composites containing Ni-Fe coated carbon nanofibers prepared by electroless plating. *Compos Part A Appl Sci Manuf*. **2011**;42(5):573–578.
- [157] Zhang T, Huang D, Yang Y, et al. $\text{Fe}_3\text{O}_4/\text{carbon}$ composite nanofiber absorber with enhanced microwave absorption performance. *Mater Sci Eng: B*. **2013**;178(1):1–9.
- [158] Wang L, He F, Wan Y. Facile synthesis and electromagnetic wave absorption properties of magnetic carbon fiber coated with Fe-Co alloy by electroplating. *J Alloys Compd*. **2011**;509(14):4726–4730.
- [159] Liu L, Zhang S, Yan F, et al. Three-dimensional hierarchical MoS_2 nanosheets/ultralong N-doped carbon nanotubes as high-performance electromagnetic wave absorbing material. *ACS Appl Mater Interfaces*. **2018**;10(16):14108–14115.
- [160] Ye Z, Li Z, Roberts JA, et al. Electromagnetic wave absorption properties of carbon nanotubes-epoxy composites at microwave frequencies. *J Appl Phys*. **2010**;108(5):054315.
- [161] Ni Q-Q, Melvin GH, Natsuki T. Double-layer electromagnetic wave absorber based on barium titanate/carbon nanotube nanocomposites. *Ceram Int*. **2015**;41(8):9885–9892.
- [162] Liu G, Wang L, Chen G, et al. Enhanced electromagnetic absorption properties of carbon nanotubes and zinc oxide whisker microwave absorber. *J Alloys Compd*. **2012**;514:183–188.
- [163] Ding D, Wang J, Yu X, et al. Dispersing of functionalized CNTs in Si-O-C ceramics and electromagnetic wave absorbing and mechanical properties of CNTs/Si-O-C nanocomposites. *Ceram Int*. **2020**;46(4):5407–5419.
- [164] Wei H, Yin X, Li X, et al. Controllable synthesis of defective carbon nanotubes/ $\text{Sc}_2\text{Si}_2\text{O}_7$ ceramic with adjustable dielectric properties for broadband high-performance microwave absorption. *Carbon*. **2019**;147:276–283.
- [165] Xu J, Xia L, Luo J, et al. The high-performance electromagnetic wave absorbing CNT/SiC_f composites: synthesis, tuning, and mechanism. *ACS Appl Mater Interfaces*. **2020**;12(18):20775–20784.
- [166] Bi S, Su X, Hou G, et al. Electrical conductivity and microwave absorption of shortened multi-walled carbon nanotube/alumina ceramic composites. *Ceram Int*. **2013**;39(5):5979–5983.
- [167] Li Y, Li Z, Shen PK. Simultaneous formation of ultra-high surface area and three-dimensional hierarchical porous graphene-like networks for fast and highly stable supercapacitors. *Adv Mater*. **2013**;25(17):2474–2480.
- [168] Cao W-Q, Wang X-X, Yuan J, et al. Temperature dependent microwave absorption of ultrathin graphene composites. *J Mater Chem C*. **2015**;3(38):10017–10022.
- [169] Worsley MA, Kucheyev SO, Mason HE, et al. Mechanically robust 3D graphene macroassembly with high surface area. *Chem Commun*. **2012**;48(67):8428–8430.
- [170] Hu H, Zhao Z, Zhou Q, et al. The role of microwave absorption on formation of graphene from graphite oxide. *Carbon*. **2012**;50(9):3267–3273.
- [171] Chen C-Y, Pu N-W, Liu Y-M, et al. Microwave absorption properties of holey graphene/silicone rubber composites. *Compos Part B Eng*. **2018**;135:119–128.
- [172] Zhang D, Jia Y, Cheng J, et al. High-performance microwave absorption materials based on MoS_2 -graphene isomorphic hetero-structures. *J Alloys Compd*. **2018**;758:62–71.
- [173] Liu X, Yu Z, Ishikawa R, et al. Single-source-precursor synthesis and electromagnetic properties of novel RGO-SiCN ceramic nanocomposites. *J Mater Chem C*. **2017**;5(31):7950–7960.
- [174] Ding D, Wang J, Xiao G, et al. Enhanced electromagnetic wave absorbing properties of Si-O-C ceramics with in-situ formed 1D nanostructures. *Int J Appl Ceram Technol*. **2019**;17(2):734–744.

- [175] Shi Y, Luo F, Ding D, et al. Effects of oxidation curing of polycarbosilane on dielectric and microwave absorption properties of PDCs-SiC ceramics. *Int J Appl Ceram Technol.* **2016**;13(1):17–22.
- [176] Ding D, Li Z, Xiao G, et al. Ku-band electromagnetic wave absorbing properties of polysiloxane derived Si-O-C bulk ceramics. *Mater Res Express.* **2018**;5(2):025039–025049.
- [177] Zhuo RF, Qiao L, Feng HT, et al. Microwave absorption properties and the isotropic antenna mechanism of ZnO nanotrees. *J Appl Phys.* **2008**;104(9):094101–094106.
- [178] Li Q, Yin X, Duan W, et al. Dielectric and microwave absorption properties of polymer derived SiCN ceramics annealed in N₂ atmosphere. *J Eur Ceram Soc.* **2014**;34(3):589–598.
- [179] Zhang T, Zhang J, Wen G, et al. Ultra-light h-BCN architectures derived from new organic monomers with tunable electromagnetic wave absorption. *Carbon.* **2018**;136:345–358.
- [180] Liu X, Zhang L, Yin X, et al. The microstructure and electromagnetic wave absorption properties of near-stoichiometric SiC fibre. *Ceram Int.* **2017**;43(3):3267–3273.
- [181] Liu R, Lun N, Qi Y-X, et al. Microwave absorption properties of TiN nanoparticles. *J Alloys Compd.* **2011**;509(41):10032–10035.
- [182] Wu R, Zhou K, Yang Z, et al. Molten-salt-mediated synthesis of SiC nanowires for microwave absorption applications. *Cryst Eng Comm.* **2013**;15(3):570–576.
- [183] Wang P, Cheng L, Zhang Y, et al. Flexible SiC/Si₃N₄ composite nanofibers with in situ embedded graphite for highly efficient electromagnetic wave absorption. *ACS Appl Mater Interfaces.* **2017**;9(34):28844–28858.
- [184] Liu L, Duan Y, Ma L, et al. Microwave absorption properties of a wave-absorbing coating employing carbonyl-iron powder and carbon black. *Appl Surf Sci.* **2010**;257(3):842–846.
- [185] Liu X, Zhang Z, Wu Y. Absorption properties of carbon black/silicon carbide microwave absorbers. *Compos Part B Eng.* **2011**;42(2):326–329.
- [186] Song W-L, Guan X-T, Fan L-Z, et al. Strong and thermostable polymeric graphene/silica textile for lightweight practical microwave absorption composites. *Carbon.* **2016**;100:109–117.
- [187] Song C, Yin X, Han M, et al. Three-dimensional reduced graphene oxide foam modified with ZnO nanowires for enhanced microwave absorption properties. *Carbon.* **2017**;116:50–58.
- [188] Cao M-S, Song W-L, Hou Z-L, et al. The effects of temperature and frequency on the dielectric properties, electromagnetic interference shielding and microwave-absorption of short carbon fiber/silica composites. *Carbon.* **2010**;48(3):788–796.
- [189] Xie S, Jin G-Q, Meng S, et al. Microwave absorption properties of in situ grown CNTs/SiC composites. *J Alloys Compd.* **2012**;520:295–300.
- [190] Mo Z, Yang R, Lu D, et al. Lightweight, three-dimensional carbon nanotube@TiO₂ sponge with enhanced microwave absorption performance. *Carbon.* **2019**;144:433–439.
- [191] Chen C, Pan L, Jiang S, et al. Electrical conductivity, dielectric and microwave absorption properties of graphene nanosheets/magnesia composites. *J Eur Ceram Soc.* **2018**;38(4):1639–1646.
- [192] Kuang J, Hou X, Xiao T, et al. Three-dimensional carbon nanotube/SiC nanowire composite network structure for high-efficiency electromagnetic wave absorption. *Ceram Int.* **2019**;45(5):6263–6267.
- [193] Huang B, Wang Z, Hu H, et al. Enhancement of the microwave absorption properties of PyC-SiC_f/SiC composites by electrophoretic deposition of SiC nanowires on SiC fibers. *Ceram Int.* **2020**;46(7):9303–9310.
- [194] Li Q, Yin X, Duan W, et al. Improved dielectric properties of PDCs-SiCN by in-situ fabricated nanostructured carbons. *J Eur Ceram Soc.* **2017**;37(4):1243–1251.
- [195] Zhang W, He X, Du Y. EMW absorption properties of in-situ growth seamless SiBCN-graphene hybrid material. *Ceram Int.* **2019**;45(1):659–664.
- [196] Chen L, Zhao J, Wang L, et al. In-situ pyrolyzed polymethylsilsesquioxane multi-walled carbon nanotubes derived ceramic nanocomposites for electromagnetic wave absorption. *Ceram Int.* **2019**;45(9):11756–11764.
- [197] Liu Y, Zeng S, Teng Z, et al. Carbon nanofibers propped hierarchical porous SiOC ceramics toward efficient microwave absorption. *Nanoscale Res Lett.* **2020**;15(1):28–35.
- [198] Ma M, Yang R, Zhang C, et al. Direct large-scale fabrication of C-encapsulated B₄C nanoparticles with tunable dielectric properties as excellent microwave absorbers. *Carbon.* **2019**;148:504–511.
- [199] Kang Y, Jiang Z, Ma T, et al. Hybrids of reduced graphene oxide and hexagonal boron nitride: light-weight absorbers with tunable and highly efficient microwave attenuation properties. *ACS Appl Mater Interfaces.* **2016**;8(47):32468–32476.
- [200] Zhang M, Li Z, Wang T, et al. Preparation and electromagnetic wave absorption performance of Fe₃Si/SiC@SiO₂ nanocomposites. *Chem Eng J.* **2019**;362:619–627.
- [201] Zhao H-B, Fu Z-B, Chen H-B, et al. Excellent electromagnetic absorption capability of Ni/carbon based conductive and magnetic foams synthesized via a green one pot route. *ACS Appl Mater Interfaces.* **2016**;8(2):1468–1477.
- [202] Qiu S, Lyu H, Liu J, et al. Facile synthesis of porous nickel/carbon composite microspheres with enhanced electromagnetic wave absorption by magnetic and dielectric losses. *ACS Appl Mater Interfaces.* **2016**;8(31):20258–20266.
- [203] Pan G, Zhu J, Ma S, et al. Enhancing the electromagnetic performance of Co through the phase-controlled synthesis of hexagonal and cubic Co nanocrystals grown on graphene. *ACS Appl Mater Interfaces.* **2013**;5(23):12716–12724.
- [204] Zhao B, Deng J, Liang L, et al. Lightweight porous Co₃O₄ and Co/CoO nanofibers with tunable impedance match and configuration-dependent microwave absorption properties. *CrystEngComm.* **2017**;19(41):6095–6106.
- [205] Deng J, Li S, Zhou Y, et al. Enhancing the microwave absorption properties of amorphous CoO nanosheet-coated Co (hexagonal and cubic phases) through interfacial polarizations. *J Colloid Interface Sci.* **2018**;509:406–413.
- [206] Ding Z, Shi SQ, Zhang H, et al. Electromagnetic shielding properties of iron oxide impregnated kenaf bast fiberboard. *Compos Part B Eng.* **2015**;78:266–271.
- [207] Tang H, Jian X, Wu B, et al. Fe₃C/helical carbon nanotube hybrid: facile synthesis and spin-induced

- enhancement in microwave-absorbing properties. *Compos Part B Eng.* **2016**;107:51–58.
- [208] Wang Y, Feng Y, Guo X, et al. Electromagnetic and wave absorbing properties of Fe-doped polymer-derived SiCN ceramics. *RSC Adv.* **2017**;7(73):46215–46220.
- [209] Yang Y, Xia L, Zhang T, et al. Fe_3O_4 @LAS/RGO composites with a multiple transmission-absorption mechanism and enhanced electromagnetic wave absorption performance. *Chem Eng J.* **2018**;352:510–518.
- [210] Li X, Gao M, Jiang Y. Synthesis and electromagnetic wave reflectivity of Si_3N_4 ceramic with gradient Fe_3O_4 distribution. *Ceram Int.* **2016**;42(8):9636–9639.
- [211] Wang Y, Guo X, Feng Y, et al. Wave absorbing performance of polymer-derived SiCN(Fe) ceramics. *Ceram Int.* **2017**;43(17):15551–15555.
- [212] Singh S, Shukla S, Kumar A, et al. Influence of Zn dispersion in SiC on electromagnetic wave absorption characteristics. *J Alloys Compd.* **2018**;738:448–460.
- [213] Liu X, Huang Y, Zhang N, et al. Synthesis of CoNi/ SiO_2 core-shell nanoparticles decorated reduced graphene oxide nanosheets for enhanced electromagnetic wave absorption properties. *Ceram Int.* **2018**;44(18):22189–22197.
- [214] Hou Y, Xiao B, Yang G, et al. Enhanced electromagnetic wave absorption performance of novel carbon-coated Fe_3Si nanoparticles in an amorphous SiCO ceramic matrix. *J Mater Chem C.* **2018**;6(28):7661–7670.
- [215] Lou Z, Li Y, Han H, et al. Synthesis of porous 3D Fe/C composites from waste wood with tunable and excellent electromagnetic wave absorption performance. *ACS Sustain Chem Eng.* **2018**;6(11):15598–15607.
- [216] Luo C, Duan W, Yin X, et al. Microwave-absorbing polymer-derived ceramics from cobalt-coordinated poly(dimethylsilylene)diacetylenes. *J Phys Chem C.* **2016**;120(33):18721–18732.
- [217] Ma Z, Wang J, Liu Q, et al. Microwave absorption of electroless Ni-Co-P-coated SiO_2 powder. *Appl Surf Sci.* **2009**;255(13–14):6629–6633.
- [218] Huang X, Zhang M, Qin Y, et al. Bead-like Co-doped ZnO with improved microwave absorption properties. *Ceram Int.* **2019**;45(6):7789–7796.
- [219] Wang S, Lin X, Ashfaq MZ, et al. Microwave absorption properties of SiCN ceramics doped with cobalt nanoparticles. *J Mater Sci Mater Electron.* **2020**;31(5):3803–3816.
- [220] Wang H, Wu L, Jiao J, et al. Covalent interaction enhanced electromagnetic wave absorption in SiC/Co hybrid nanowires. *J Mater Chem A.* **2015**;3(12):6517–6525.
- [221] Liang C, Liu C, Wang H, et al. SiC- Fe_3O_4 dielectric-magnetic hybrid nanowires: controllable fabrication, characterization and electromagnetic wave absorption. *J Mater Chem A.* **2014**;2(39):16397–16402.
- [222] Sun M, Lv X, Xie A, et al. Growing 3D ZnO nanocrystals on 1D SiC nanowires: enhancement of dielectric properties and excellent electromagnetic absorption performance. *J Mater Chem C.* **2016**;4(38):8897–8902.
- [223] Kuang J, Jiang P, Liu W, et al. Synergistic effect of Fe-doping and stacking faults on the dielectric permittivity and microwave absorption properties of SiC whiskers. *Appl Phys Lett.* **2015**;106(21–25):212903.
- [224] Singh S, Kumar A, Agarwal S, et al. Synthesis and tunable microwave absorption characteristics of flower-like Ni/SiC composites. *J Magn Magn Mater.* **2020**;503:166616–166626.
- [225] Kuang J, Xiao T, Zheng Q, et al. Dielectric permittivity and microwave absorption properties of transition metal Ni and Mn doped SiC nanowires. *Ceram Int.* **2020**;46(9):12996–13002.
- [226] Wei B, Zhou J, Yao Z, et al. The effect of Ag nanoparticles content on dielectric and microwave absorption properties of β -SiC. *Ceram Int.* **2020**;46(5):5788–5798.
- [227] Liu Y, Lin X, Gong H, et al. Electromagnetic properties and microwave absorption performances of nickel-doped SiCN ceramics pyrolyzed at different temperatures. *J Alloys Compd.* **2019**;771:356–363.
- [228] Du B, Qian J, Hu P, et al. Enhanced electromagnetic wave absorption of Fe-doped silicon oxycarbide nanocomposites. *J Am Ceram Soc.* **2020**;103(3):1732–1743.
- [229] Liu Y, Luo F, Su J, et al. Electromagnetic and microwave absorption properties of the nickel/Ti₃SiC₂ hybrid powders in X-band. *J Magn Magn Mater.* **2014**;365:126–131.
- [230] Li Z, Yang Z, Zhang M, et al. Dielectric properties of Al-doped Ti₃SiC₂ as a novel microwave absorbing material. *Ceram Int.* **2017**;43(1, Part A):222–227.
- [231] Javid M, Zhou Y, Wang D, et al. Strong microwave absorption of Fe@ SiO_2 nanocapsules fabricated by one-step high energy plasma. *J Phys Chem Solids.* **2019**;129:242–251.
- [232] Hou Y, Xiao B, Sun Z, et al. High temperature anti-oxidative and tunable wave absorbing SiC/ Fe_3Si /CNTs composite ceramic derived from a novel polysilyacetylene. *Ceram Int.* **2019**;45(13):16369–16379.
- [233] Liu P, Huang Y, Yan J, et al. Magnetic graphene@PANI@porous TiO₂ ternary composites for high-performance electromagnetic wave absorption. *J Mater Chem C.* **2016**;4(26):6362–6370.
- [234] Zhou P, Chen J-h, Liu M, et al. Microwave absorption properties of SiC@ SiO_2 @ Fe_3O_4 hybrids in the 2–18 GHz range. *Int J Miner Metall Mater.* **2017**;24(7):804–813.
- [235] Wang L, Zhu J, Yang H, et al. Fabrication of hierarchical graphene@ Fe_3O_4 @ SiO_2 @polyaniline quaternary composite and its improved electrochemical performance. *J Alloys Compd.* **2015**;634:232–238.
- [236] Ren Y-L, Wu H-Y, Lu M-M, et al. Quaternary nanocomposites consisting of graphene, Fe_3O_4 @Fe Core@Shell, and ZnO nanoparticles: synthesis and excellent electromagnetic absorption properties. *ACS Appl Mater Interfaces.* **2012**;4(12):6436–6442.
- [237] Chen Y-H, Huang Z-H, Lu M-M, et al. 3D Fe_3O_4 nanocrystals decorating carbon nanotubes to tune electromagnetic properties and enhance microwave absorption capacity. *J Mater Chem A.* **2015**;3(24):12621–12625.
- [238] Wang L, Huang Y, Sun X, et al. Synthesis and microwave absorption enhancement of graphene@ Fe_3O_4 @ SiO_2 @NiO nanosheet hierarchical structures. *Nanoscale.* **2014**;6(6):3157–3164.
- [239] Sun D, Zou Q, Wang Y, et al. Controllable synthesis of porous Fe_3O_4 @ZnO sphere decorated graphene for extraordinary electromagnetic wave absorption. *Nanoscale.* **2014**;6(12):6557–6562.
- [240] Wang L, Huang Y, Li C, et al. Hierarchical composites of polyaniline nanorod arrays covalently-grafted

- on the surfaces of graphene@Fe₃O₄@C with high microwave absorption performance. *Compos Sci Technol.* **2015**;108:1–8.
- [241] Singh S, Maurya AK, Gupta R, et al. Improved microwave absorption behavioral response of Ni/SiC and Ni/SiC/graphene composites: a comparative insight. *J Alloys Compd.* **2020**;823:153780–153792.
- [242] Wang P, Liu P-A, Ye S. Preparation and microwave absorption properties of Ni(Co/Zn/Cu)Fe₂O₄/SiC@SiO₂ composites. *Rare Met.* **2019**;38(1):59–63.
- [243] He J, Deng L, Luo H, et al. Electromagnetic matching and microwave absorption abilities of Ti₃SiC₂ encapsulated with Ni_{0.5}Zn_{0.5}Fe₂O₄ shell. *J Magn Magn Mater.* **2019**;473:184–189.
- [244] Zhang Y, Meng H, Shi Y, et al. Tin/Ni/C ternary composites with expanded heterogeneous interfaces for efficient microwave absorption. *Compos Part B Eng.* **2020**;193:108028–108036.
- [245] Pang H, Pang W, Zhang B, et al. Excellent microwave absorption properties of the h-BN-GO-Fe₃O₄ ternary composite. *J Mater Chem C.* **2018**;6(43):11722–11730.
- [246] Liu Y, Jian X, Su X, et al. Electromagnetic interference shielding and absorption properties of Ti₃SiC₂/nano Cu/epoxy resin coating. *J Alloys Compd.* **2018**;740:68–76.
- [247] Kong L, Yin X, Zhang L, et al. Effect of aluminum doping on microwave absorption properties of ZnO/ZrSiO₄ composite ceramics. *J Am Ceram Soc.* **2012**;95(10):3158–3165.
- [248] Liu X, Chai N, Yu Z, et al. Ultra-light, high flexible and efficient CNTs/Ti₃C₂-sodium alginate foam for electromagnetic absorption application. *J Mater Sci Technol.* **2019**;35(12):2859–2867.
- [249] Zhao B, Zhao W, Shao G, et al. Morphology-control synthesis of a core-shell structured NiCu alloy with tunable electromagnetic-wave absorption capabilities. *ACS Appl Mater Interfaces.* **2015**;7(23):12951–12960.
- [250] Zhao B, Fan B, Xu Y, et al. Preparation of honeycomb SnO₂ foams and configuration-dependent microwave absorption features. *ACS Appl Mater Interfaces.* **2015**;7(47):26217–26225.
- [251] Zhao B, Guo X, Zhao W, et al. Yolk-Shell Ni@SnO₂ composites with a designable interspace to improve the electromagnetic wave absorption properties. *ACS Appl Mater Interfaces.* **2016**;8(42):28917–28925.
- [252] Zhu Q, Zhang Z, Lv Y, et al. Synthesis and electromagnetic wave absorption performance of NiCo₂O₄ nanomaterials with different nanostructures. *CrystEngComm.* **2019**;21(31):4568–4577.
- [253] Yuan X, Wang R, Huang W, et al. Lamellar vanadium nitride nanowires encapsulated in graphene for electromagnetic wave absorption. *Chem Eng J.* **2019**;378:122203–122213.
- [254] Wu H, Liu J, Liang H, et al. Sandwich-like Fe₃O₄/Fe₃S₄ composites for electromagnetic wave absorption. *Chem Eng J.* **2020**;393:124743.
- [255] Zhao B, Shao G, Fan B, et al. In situ synthesis of novel urchin-like ZnS/Ni₃S₂@Ni composite with a core-shell structure for efficient electromagnetic absorption. *J Mater Chem C.* **2015**;3(41):10862–10869.
- [256] Su T, Zhao B, Fan B, et al. Enhanced microwave absorption properties of novel hierarchical core-shell δ/α MnO₂ composites. *J Solid State Chem.* **2019**;273:192–198.
- [257] Yudistira HT. Tailoring multiple reflections by using graphene as background for tunable terahertz meta-material absorber. *Mater Res Express.* **2019**;6(7):075804–075812.
- [258] Zhao B, Shao G, Fan B, et al. Synthesis of flower-like CuS hollow microspheres based on nanoflakes self-assembly and their microwave absorption properties. *J Mater Chem A.* **2015**;3(19):10345–10352.
- [259] Pan J, Xia W, Sun X, et al. Improvement of interfacial polarization and impedance matching for two-dimensional leaf-like bimetallic (Co, Zn) doped porous carbon nanocomposites with broadband microwave absorption. *Appl Surf Sci.* **2020**;512:144894–144904.
- [260] Yang L, Lv H, Li M, et al. Multiple polarization effect of shell evolution on hierarchical hollow C@MnO₂ composites and their wideband electromagnetic wave absorption properties. *Chem Eng J.* **2020**;392:123666–123676.
- [261] Elahi A, Shakoor A, Irfan M, et al. Effect of loading ZnNiCrFe₂O₄ nanoparticles on structural and microwave absorption properties of polyaniline nanocomposites. *J Mater Sci Mater Electron.* **2016**;27(9):9489–9495.
- [262] Bueno AR, Gregori ML, Nóbrega MCS. Microwave-absorbing properties of Ni_{0.50-x}Zn_{0.50-x}Me_{2x}Fe₂O₄ (Me=Cu, Mn, Mg) ferrite-wax composite in X-band frequencies. *J Magn Magn Mater.* **2008**;320(6):864–870.
- [263] Zhang L, Zhu H, Song Y, et al. The electromagnetic characteristics and absorbing properties of multi-walled carbon nanotubes filled with Er₂O₃ nanoparticles as microwave absorbers. *Mater Sci Eng B.* **2008**;153(1):78–82.
- [264] Lv H, Liang X, Ji G, et al. Porous three-dimensional flower-like Co/CoO and its excellent electromagnetic absorption properties. *ACS Appl Mater Interfaces.* **2015**;7(18):9776–9783.
- [265] Fang J, Liu T, Chen Z, et al. A wormhole-like porous carbon/magnetic particles composite as an efficient broadband electromagnetic wave absorber. *Nanoscale.* **2016**;8(16):8899–8909.
- [266] Wang F, Sun Y, Li D, et al. Microwave absorption properties of 3D cross-linked Fe/C porous nanofibers prepared by electrospinning. *Carbon.* **2018**;134:264–273.
- [267] Sun D, Zou Q, Qian G, et al. Controlled synthesis of porous Fe₃O₄-decorated graphene with extraordinary electromagnetic wave absorption properties. *Acta Mater.* **2013**;61(15):5829–5834.
- [268] Yin X, Xue Y, Zhang L, et al. Dielectric, electromagnetic absorption and interference shielding properties of porous yttria-stabilized zirconia/silicon carbide composites. *Ceram Int.* **2012**;38(3):2421–2427.
- [269] Lin Y, Dai J, Yang H, et al. Graphene multilayered sheets assembled by porous Bi₂Fe₄O₉ microspheres and the excellent electromagnetic wave absorption properties. *Chem Eng J.* **2018**;334:1740–1748.
- [270] Feng J, Zong Y, Sun Y, et al. Optimization of porous FeNi₃/N-GN composites with superior microwave absorption performance. *Chem Eng J.* **2018**;345:441–451.
- [271] Liu L, Duan Y, Guo J, et al. Influence of particle size on the electromagnetic and microwave absorption properties of FeSi/paraffin composites. *Phys B.* **2011**;406(11):2261–2265.

- [272] Wu LZ, Ding J, Jiang HB, et al. Particle size influence to the microwave properties of iron based magnetic particulate composites. *J Magn Magn Mater.* **2005**;285(1):233–239.
- [273] Wu N, Liu X, Zhao C, et al. Effects of particle size on the magnetic and microwave absorption properties of carbon-coated nickel nanocapsules. *J Alloys Compd.* **2016**;656:628–634.
- [274] Zhou PH, Deng LJ, Xie JL, et al. Nanocrystalline structure and particle size effect on microwave permeability of FeNi powders prepared by mechanical alloying. *J Magn Magn Mater.* **2005**;292:325–331.
- [275] Wang C, Lv R, Huang Z, et al. Synthesis and microwave absorbing properties of FeCo alloy particles/graphite nanoflake composites. *J Alloys Compd.* **2011**;509(2):494–498.
- [276] Wang D-J, Zhang J-Y, He P, et al. Size-modulated electromagnetic properties and highly efficient microwave absorption of magnetic iron oxide ceramic opened-hollow microspheres. *Ceram Int.* **2019**;45(17, Part B):23043–23049.
- [277] Chen N, Jiang JT, Xu CY, et al. Co₇Fe₃ and Co₇Fe₃@SiO₂ nanospheres with tunable diameters for high-performance electromagnetic wave absorption. *ACS Appl Mater Interfaces.* **2017**;9(26):21933–21941.
- [278] Ghanbari F, Moradi Dehaghi S, Mahdavi H. Epoxy-based multilayered coating containing carbon nanotube (CNT), silicon carbide (SiC), and carbonyl iron (CI) particles: as efficient microwave absorbing materials. *J Coat Technol Res.* **2020**;17:815–826.
- [279] Li X, Zhang L, Yin X. Electromagnetic properties of pyrolytic carbon-Si₃N₄ ceramics with gradient PyC distribution. *J Eur Ceram Soc.* **2013**;33(4):647–651.
- [280] Li Z-J, Shi G-M, Zhao Q. Improved microwave absorption properties of core-shell type Ni@SiC nanocomposites. *J Mater Sci Mater Electron.* **2017**;28(8):5887–5897.
- [281] Zhou S, Huang Y, Liu X, et al. Synthesis and microwave absorption enhancement of CoNi@SiO₂@C hierarchical structures. *Ind Eng Chem Res.* **2018**;57(16):5507–5516.
- [282] Liu Y, Wu W-W, Liu L-N, et al. Heterointerface engineering of lightweight, worm-like SiC/B₄C hybrid nanowires as excellent microwave absorbers. *J Mater Chem C.* **2019**;7(32):9892–9899.
- [283] Wang X, Yin L, Chen C, et al. Synthesis of tremella-like graphene@SiC nano-structure for electromagnetic wave absorbing material application. *J Alloys Compd.* **2018**;741:205–210.
- [284] Luo H, Xiao P, Huang L, et al. Dielectric properties of C_f-Si₃N₄ sandwich composites prepared by gelcasting. *Ceram Int.* **2014**;40(6):8253–8259.
- [285] Ren Y, Zhu C, Zhang S, et al. Three-dimensional SiO₂@Fe₃O₄ core/shell nanorod array/graphene architecture: synthesis and electromagnetic absorption properties. *Nanoscale.* **2013**;5(24):12296–12303.
- [286] Li B, Mao B, He T, et al. Effect of SiC layer on microwave absorption properties of novel three-dimensional interconnected SiC foam with double-layer hollow skeleton. *Mater Res Express.* **2020**;7(1):015073–015087.
- [287] Du B, Qian J, Hu P, et al. Fabrication of C-doped SiC nanocomposites with tailoring dielectric properties for the enhanced electromagnetic wave absorption. *Carbon.* **2020**;157:788–795.
- [288] Wei B, Zhou J, Yao Z, et al. Excellent microwave absorption property of nano-Ni coated hollow silicon carbide core-shell spheres. *Appl Surf Sci.* **2020**;508:145261–145274.
- [289] Liu T, Liu N, Zhai S, et al. Tailor-made core/shell/shell-like Fe₃O₄@SiO₂@PPy composites with prominent microwave absorption performance. *J Alloys Compd.* **2019**;779:831–843.
- [290] Xiao S, Mei H, Han D, et al. Sandwich-like SiCnw/C/Si₃N₄ porous layered composite for full X-band electromagnetic wave absorption at elevated temperature. *Compos Part B Eng.* **2020**;183:107629–107663.
- [291] Dong Y, Yin X, Wei H, et al. Carbon nanowires reinforced porous SiO₂/3Al₂O₃·2SiO₂ ceramics with tunable electromagnetic absorption properties. *Ceram Int.* **2019**;45(9):11316–11324.
- [292] Li X-P, Deng Z, Li Y, et al. Controllable synthesis of hollow microspheres with Fe@carbon dual-shells for broad bandwidth microwave absorption. *Carbon.* **2019**;147:172–181.
- [293] Jiang Y, Chen Y, Liu Y-J, et al. Lightweight spongy bone-like graphene@SiC aerogel composites for high-performance microwave absorption. *Chem Eng J.* **2018**;337:522–531.
- [294] Zhong B, Sai T, Xia L, et al. High-efficient production of SiC/SiO₂ core-shell nanowires for effective microwave absorption. *Mater Des.* **2017**;121:185–193.
- [295] Rong H, Zhang Z, Li Y, et al. Significant magnetocaloric and microwave absorption performances in ultrafine ErC₂@C core-shell structural nanocomposites. *Compos Commun.* **2019**;12:123–127.
- [296] Ye X, Chen Z, Ai S, et al. Synthesis and microwave absorption properties of novel reticulation SiC/porous melamine-derived carbon foam. *J Alloys Compd.* **2019**;791:883–891.
- [297] Yang HJ, Cao WQ, Zhang DQ, et al. NiO hierarchical nanorings on SiC: enhancing relaxation to tune microwave absorption at elevated temperature. *ACS Appl Mater Interfaces.* **2015**;7(13):7073–7078.
- [298] Yuan J, Yang H-J, Hou Z-L, et al. Ni-decorated SiC powders: enhanced high-temperature dielectric properties and microwave absorption performance. *Powder Technol.* **2013**;237:309–313.
- [299] Mu Y, Zhou W, Hu Y, et al. Temperature-dependent dielectric and microwave absorption properties of SiC_f/SiC-Al₂O₃ composites modified by thermal cross-linking procedure. *J Eur Ceram Soc.* **2015**;35(11):2991–3003.
- [300] Kuang B, Dou Y, Wang Z, et al. Enhanced microwave absorption properties of Co-doped SiC at elevated temperature. *Appl Surf Sci.* **2018**;445:383–390.
- [301] Yuan X, Cheng L, Zhang Y, et al. Fe-doped SiC/SiO₂ composites with ordered inter-filled structure for effective high-temperature microwave attenuation. *Mater Des.* **2016**;92:563–570.
- [302] Han T, Luo R, Cui G, et al. Effect of SiC nanowires on the high-temperature microwave absorption properties of SiC_f/SiC composites. *J Eur Ceram Soc.* **2019**;39(5):1743–1756.
- [303] Luo C, Jiao T, Tang Y, et al. Excellent electromagnetic wave absorption of iron-containing SiBCN ceramics at 1158 K high-temperature. *Adv Eng Mater.* **2018**;20(6):1701168–1701178.
- [304] Xu H, Yin X, Li M, et al. Mesoporous carbon hollow microspheres with red blood cell like morphology for efficient microwave absorption at elevated temperature. *Carbon.* **2018**;132:343–351.

- [305] Liu J, Cao M-S, Luo Q, et al. Electromagnetic property and tunable microwave absorption of 3D nets from nickel chains at elevated temperature. *ACS Appl Mater Interfaces*. 2016;8(34):22615–22622.
- [306] Kong L, Yin X, Li Q, et al. High-temperature electromagnetic wave absorption properties of ZnO/ZrSiO₄ composite ceramics. *J Am Ceram Soc*. 2013;96(7):2211–2217.
- [307] Lu M, Wang X, Cao W, et al. Carbon nanotube-CdS core-shell nanowires with tunable and high-efficiency microwave absorption at elevated temperature. *Nanotechnology*. 2015;27(6):065702–065709.
- [308] Han M, Yin X, Duan W, et al. Hierarchical graphene/SiC nanowire networks in polymer-derived ceramics with enhanced electromagnetic wave absorbing capability. *J Eur Ceram Soc*. 2016;36(11):2695–2703.
- [309] Yang H-J, Cao W-Q, Zhang D-Q, et al. NiO hierarchical nanorings on SiC: enhancing relaxation to tune microwave absorption at elevated temperature. *ACS Appl Mater Interfaces*. 2015;7(13):7073–7077.
- [310] Kong L, Yin X, Han M, et al. Carbon nanotubes modified with ZnO nanoparticles: high-efficiency electromagnetic wave absorption at high-temperatures. *Ceram Int*. 2015;41(3, Part B):4906–4915.
- [311] Peng C-H, Shiu Chen P, Chang C-C. High-temperature microwave bilayer absorber based on lithium aluminum silicate/lithium aluminum silicate-SiC composite. *Ceram Int*. 2014;40(1, Part A):47–55.
- [312] Dong S, Hu P, Zhang X, et al. Carbon foams modified with in-situ formation of Si₃N₄ and SiC for enhanced electromagnetic microwave absorption property and thermostability. *Ceram Int*. 2018;44(6):7141–7150.
- [313] Xiao S, Mei H, Han D, et al. Ultralight lamellar amorphous carbon foam nanostructured by SiC nanowires for tunable electromagnetic wave absorption. *Carbon*. 2017;122:718–725.
- [314] Zhao W, Shao G, Jiang M, et al. Ultralight polymer-derived ceramic aerogels with wide bandwidth and effective electromagnetic absorption properties. *J Eur Ceram Soc*. 2017;37(13):3973–3980.
- [315] Shao G, Liang J, Zhao W, et al. Co decorated polymer-derived SiCN ceramic aerogel composites with ultrabroad microwave absorption performance. *J Alloys Compd*. 2020;813:152007–115216.
- [316] Zhao H-B, Fu Z-B, Liu X-Y, et al. Magnetic and conductive Ni/carbon aerogels toward high-performance microwave absorption. *Ind Eng Chem Res*. 2017;57(1):202–211.